UNIVERSIDAD DE CHILE -FACULTAD DE CIENCIAS -ESCUELA DE PREGRADO

"Towards a bioleaching biofilm image analysis platform: Semi-automatic quantification of biofilm development on pyrite by differential cell labeling."

Seminario de Título entregado a la Universidad de Chile en cumplimiento parcial de los requisitos para optar al Título de Ingeniero en Biotecnología Molecular

# Francisco Osorio Kirhman

Director del Seminario de Título: Dr. Mario Vera Véliz
Profesor patrocinante: Dr. Nicolas Giuliani

Diciembre, 2020
Santiago-Chile

# INFORME DE APROBACIÓN SEMINARIO DE TITULO

Se informa a la Escuela de Pregrado de la Facultad de Ciencias, de la Universidad de Chile que el Seminario de Título, presentado por el **Sr. Francisco Osorio Kirhman:**

**"Towards a bioleaching biofilm image analysis platform: Semi-automatic quantification of biofilm development on pyrite by differential cell labeling"**

Ha sido aprobado por la Comisión de Evaluación, en cumplimiento parcial de los requisitos para optar al Título de ……………………………………….

Dr. Mario Vera

**Director Seminario de Título:** _____

**Comisión Revisora y Evaluadora:**

Dr. Francisco Chávez

**Presidente Comisión:** _____

Dra. Julieta Orlando

**Evaluador:** _____

Santiago de Chile, ………………………

**Agradecimientos.**

Terminada esta etapa miro hacia atrás a toda la gente que me ha ayudado y acompañado, y la primera persona en la que pienso es mi mamá. Nunca terminaré de agradecerte tu apoyo incondicional, los valores que me has enseñado, tu cariño y la confianza que me has tenido, gracias a ti soy la persona que soy hoy. Tengo mucha suerte de tenerte como mamá. También quiero agradecer a mis abuelos, especialmente a mi abuela Mónica, por su cariño incondicional, su entrega y los almuerzos en familia, espero que haya muchos más.

También agradezco el apoyo de mi profesor guía, Dr. Mario Vera, quién no solo me guío enseñándome de ciencia, sino que además fue una guía tanto en el trabajo de laboratorio como en el trabajo escrito, dándose el tiempo y la paciencia de enseñarme como escribir un artículo científico.

A todos aquellos que me acompañaron en mi trabajo en laboratorio en el Instituto de Ingeniería Biológica y Médica, especialmente a Christopher Holmes y Sergio Itier por sus charlas científicas. A Camila Cárdenas por guiarme y enseñarme como trabajar con bacterias y biofilms, aprendí mucho en esas tardes siendo minion y espero que la ciencia nos lleve a más proyectos juntos. A Cristian Jorquera, por enseñarme a usar el EFM y por supuesto por nuestras charlas científicas que no se detuvieron a pesar de la distancia, te deseo lo mejor amigo, en Alemania y en la vida. A Francisca Bugueño por tenerme paciencia, enseñarme a trabajar ordenadamente y ayudarme con los protocolos. A Beatriz Salas, por ser un ejemplo a seguir, enseñarme a trabajar en mesón y responder mis múltiples dudas durante la escritura de este trabajo.

A María José Vásquez Pino, por acompañarme en escribir, enseñarme de la vida y recibirme en su casa, todo en una pandemia mundial. Estar contigo hizo de la cuarentena algo nuevo todos los días. Espero que logres todo lo que te propones, gracias por ser parte de mi vida.

A mis amigos por acompañarme en este camino, por lo buenos momentos haciendo trabajos juntos y por enseñarme. Queda mucha gente más a la que agradecer, pero me faltarían páginas, espero se les devuelva todo el bien que me han hecho en la vida.

También agradecer a Timothy Rudge, Isaac Nuñez y Beatriz Salas, por amablemente proveer el software personalizado usado, además de fotos de *L. ferriphilum* y *L. ferrooxidans*, respectivamente. A Arnaud Kolzner por su ayuda en el análisis con Fiji.

UNIVERSIDAD DE CHILE - FACULTAD DE CIENCIAS - ESCUELA DE PREGRADO

UNIVERSIDAD DE CHILE - FACULTAD DE CIENCIAS - ESCUELA DE PREGRADO

Abbreviations.

AI: Auto Inducer.
AMD: Acid Mine Drainage.
ARD: Acid Rock Drainage.
BDSF: *cis*-2-dodecenoic acid.
BF: Biofilm.
ConA: Concanavalin A.
DAPI: 4′,6-diamidino-2-phenylindole.
DilC: 1,1'-dioctadecyl-6,6'- di(4-sulfophenyl)-3,3, 3',3'-tetramethylindocarbocyanine.
DiO: 3,3'-dioctadecyl-5,5'- di(4-sulfophenyl) oxacarbocyanine, sodium salt.
DMSO: Dimethyl sulfoxide.
DNA: Deoxyribonucleic Acid.
DSF: *cis*-11-methyl-dodecenoic acid.
DSF: Diffusible Signaling Factor.
eDNA: extracellular DNA.
EFM: Epifluorescence Microscopy.
EPS: Extracellular Polymeric Substances.
Fm-dye: Fei Mao dye.
Gt: Gigaton.
HSL: N-Acyl Homoserine Lactone.
$C_{12}$-HSL: N-dodecanoyl-homoserine lactone.
O-$C_{12}$-HSL: N-3-dodecanoyl-homoserine lactone.
$C_{14}$-HSL: N-tetradecanoyl-homoserine lactone.
O-$C_{14}$-HSL: N-3-tetradecanoyl-homoserine lactone.
qPCR: quantitative Polymerase Chain Reaction.
QS: Quorum Sensing.
MS: Metal Sulfide.
Mt:  Megaton.
RISC: Reduced Inorganic Sulfur Compounds.
ROS: Reactive Oxygen Species.
*rpf*: regulation of pathogenicity.
SD: Standard Deviation.

**1 Abstract.**

Leaching microorganisms catalyze the dissolution of metal sulfides (MS) by attaching to mineral surfaces and producing extracellular polymeric substances (EPS), which among other characteristics, allows an efficient leaching of the mineral. Attachment to MS is affected by diverse factors, such as growth conditions, the previous/present presence of other colonizers or their EPS, cell-to-cell communication mechanisms, among others. In natural environments biofilms (BF) form as complex communities with multispecies interactions. Further insights in the study of BF development could help to improve the comprehension of interactions between different colonizing species in the mineral surface, however BFs are generally composed by a mixture of microorganisms, therefore, non- invasive BF analysis tools have to be further developed to allow species-specific recognition of cells in BF images. Bacteria are heterogeneously distributed in pyrite grains, therefore strategies such as, the analysis of large sets of BF images, are implemented to try to overcome this difficulty. A first step towards this objective is to recognize cells in axenic cultures.

In this work BFs of acidophilic bacterial species were studied using epifluorescence microscopy (EFM) and three image analysis software packages. EFM images were acquired from pyrite samples with BFs formed on the mineral surface under different conditions, BFs of *Acidiferrobacter* sp. SP3/III *Leptospirillum ferrooxidans*<sup>T</sup> and *Leptospirillum ferriphilum*<sup>T</sup> were studied. The signal spots from 480 images were quantified by using semi-automatic software.

Lipophilic membrane dyes are fluorophores composed by a polar head and two hydrophobic alkyl chains with affinity for hydrophobic solvents, when the membrane dye is incorporated into a lipid membrane it produces enhanced fluorescence. The use of membrane cell tracing dyes may be used to follow up BF development, since it has the advantage to distinguish some species in mixed cultures, even when sizes and shapes of these are similar, by differential staining and counter-staining with DNA-binding dyes, however a relation between the quantified signal from lipophilic membrane dyes and mineral attached cells visualized by DNA-binding dyes, has not been defined.

A comparison of the image analysis software packages: Zen 3.0, Fiji and a custom-made script was performed, obtaining similar relative quantification. It was found that the custom script obtained lowest quantification results, while Zen 3.0 identifies a higher number of colonies than the other 2 software for the same images. This is explained by the manual selection of the colonies step, that Zen 3.0 allows.

Finally, the custom script was used to quantify the effect of the addition of synthetic QS signal molecules acyl-homoserine lactones (HSL) and diffusible signaling factors (DSF) on BF formation and cell dispersion. Interestingly, in *L. ferrooxidans*[T] HSLs external addition of 1 mM mixtures of C12-HSL & O-C12-HSL or C14-HSL & O-C14-HSL reduced the number of attached cells on pyrite grains at 70 h, while for *L. ferriphilum*[T] the attachment at 48 h diminished upon the addition of 1 mM mixtures of C12-HSL & O-C12-HSL or 1 mM O-C14-HSL. Changes in the pattern of dispersion or attachment were not possible to be measured upon DSF addition, given the current sample size.

## 2. Introduction.

### 2.1 Biomining in Chile.

The mining industry has a huge impact in Chilean economy, being responsible for over 9.4 % of the Chilean GDP and a vast variety of direct and indirect employment. Chile with a production of 5,79 Mt of copper in 2019, is the main producer globally (Cochilco, 2019). It is predicted that copper demand will keep rising due to the vast variety of uses and applications of this mineral, the opening of new markets and the development of the already existing ones (Cochilco, 2017a).

Mining operations have a huge, and mostly irreversible, environmental impact with a generation of solid waste of over 100 Gt per year globally for the primary production of common minerals and metal goods (Tayebi-Khorami et al., 2019). A common technique used for recovery of valuable metals is pyrometallurgy, that allows high reaction rates due to the use of elevated temperatures and a high metal concentration in processing streams, however, it is becoming increasingly expensive as a result of the environmental impact associated, and the decrease of valuable ore content in the extracted rock. Also, the stock of mine waste if not managed properly, generates environmental related problems such as acid mine/rock drainage (AMD/ARD), caused by the exposition of ores containing metal sulfide (MS), mainly pyrite, the most ubiquitous of all sulfide minerals present in ore bodies, to water. Subsequent MS oxidation by microorganisms, produces an acidic leachate with high concentrations of sulfate, iron, and heavy metals that is detrimental to aquatic ecosystems and fresh water supply (Simate & Ndlovu, 2014), resulting in long-term problems with a costly remediation calculated in US$1.5 billion per year globally (Tayebi-Khorami et al., 2019).

The current Chilean legislation advances towards environmentally friendly measures such as: glacier and wetland protection, and energy efficiency reports for big consumers, such as the mining industry (Cochilco, 2019). An environmentally friendly mining industry included in a model of circular economy requires an efficient management of the available resources in a long-term strategy, aiming for reduction and/or reuse of waste and by-products. A sustainable model that simultaneously creates economic value, requires developments in re-processing of mine waste, allowing its valorization through cost effective techniques (Tayebi-Khorami et al., 2019).

Biomining, i.e., the use of acidophilic leaching microorganisms for the solubilization of valuable metals, is a technique that allows the extraction of metals from waste or low-grade ores. It is currently used for extracting 18-20 % and about 3 % of the global copper and gold production, respectively (Lakshmanan et al., 2016). Acidophilic microorganisms, i.e., microorganisms whose growth is optimal at pH values below 3, derive energy from iron (II) ions and reduced inorganic sulfur compounds (RISC), and are commonly used and found in biomining operations. These microorganisms grow chemolithoautotrophically or mixotrophically and are adapted to thrive in harsh conditions. Microbial enhanced oxidation of MS can occur between 20 °C to 40 °C for mesophilic microorganisms, but due to the exothermic nature of the leaching process heaps can vary greatly in temperature (Brierley & Brierley, 2013; Watling, 2016). This process has been subject of intensive research, as *in situ* bioleaching has lower costs than conventional mining methods for low-grade copper deposits processing, e.g., pyrometallurgical processing, and a lower carbon footprint (Johnson, 2015).
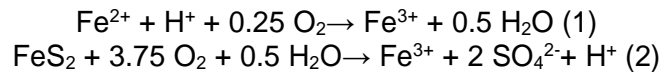
The average percentage of copper content in mined ores has declined globally (Crowson, 2012), however this trend has been especially acute in Chile, as the copper ore grade has fallen below the world average, reaching 0.65 % in 2016 (Cochilco, 2017b). Conventional methods that produce harmful gaseous emissions, such as smelting or roasting, are too energy demanding (Rawlings, 2002), and not efficient for low grade ore processing (Johnson & Hallberg, 2008). This is due to the fact that as much as the 97 % of the extracted material (for copper ore containing 1 % copper as chalcopyrite) is gangue non-valuable minerals, that needs to be separated and disposed (Lakshmanan et al., 2016; Cochilco, 2017b). Considering the trend in environmental regulations, biomining acquires importance as a technique for the processing of tailings and low-grade ores so far discarded by the mining industry.

## 2.2 Bioleaching.

Bioleaching has been used throughout history by civilizations like Greek or Romans (Bosecker, 1997), however further comprehension of its subjacent mechanisms has occurred only recently. Bioleaching is a low energy requiring method, with zero production of noxious gases, it occurs as a result of mineral oxidation by diverse organisms, whose natural habitat is MS and obtain their energy through mineral oxidation, such as fungi, bacteria or archaea (Johnson & Hallberg, 2008). In bioleaching valuable metals are solubilized and extracted through bacterial oxidation, contrarily to bio-oxidation were metal solubilization is only used for the removal of interfering non-valuable MS, preceding other treatments (as cyanidation for gold) (Rohwerder 2003).

Two main MS oxidation mechanisms are described: the thiosulfate and the polysulfide pathways. The first mechanism occurs in $FeS_2$ (pyrite), $MoS_2$ (molybdenum disulfide),

and $WS_2$ (tungsten disulfide), this reaction starts with an initial iron (III) ion mediated oxidation of the MS and thereby producing its reduction to iron (II) ions, and the release of metal cations ($M^{+2}$) to the solution (Sand et al., 2001), being thiosulfate its first soluble compound intermediate, iron (III) ions regeneration is a slow abiotic process, but is performed by numerous iron-oxidizing species, a reaction (1) that consumes oxygen and protons. However, protons are replenished as a result of RISC oxidation, reaction (2) with a net acid generation (Sand et al., 2001).

$$Fe^{2+} + H^+ + 0.25\ O_2 \rightarrow Fe^{3+} + 0.5\ H_2O \quad (1)$$
$$FeS_2 + 3.75\ O_2 + 0.5\ H_2O \rightarrow Fe^{3+} + 2\ SO_4^{2-} + H^+ \quad (2)$$

The aforementioned leaching mechanism would correspond to an "indirect mechanism" (Sand et al., 2004), in contrast to contact leaching, were anodic and cathodic reactions occur as a result of BF formation (Zhang et al., 2016).


The second MS oxidation mechanism is the polysulfide pathway, that occurs via proton cleavage of the metal-sulfur bonds, producing elemental sulfur and iron (II), this is true for MS such as: $As_4S_4$ (pararealgar), $CuFeS_2$ (chalcopyrite), FeS (pyrrhotite), $Fe_7S_8$ (pyrrhotite-4C), $MnS_2$ (manganese sulfide), PbS (lead sulfide), and ZnS (zinc sulfide) (Rohwerder et al., 2003).


## 2.3 Leaching species and their characteristics.

As mentioned, leaching microorganisms use inorganic compounds as an energy source. They are able to oxidize iron (II) ions to iron (III) ions as an energy source. *Leptospirillum ferrooxidans[T]* is an acidophilic iron-oxidizing, chemolithoautrophic Gram-negative bacterium that thrives in mesophilic environments and is abundantly present in

bioleaching heaps (Sand et al., 1992), its size ranges 0.3 µm to 0.5 µm (Coram & Rawlings, 2002). It has been postulated that its prevalence in leaching heaps is a consequence of its capability to oxidize iron (II) ions at high redox potentials (up to +950 mV, vs standard hydrogen electrode) (Rohwerder et al., 2003). *Leptospirillum ferriphilum$^T$* is another Gram-negative iron oxidizer; it grows at temperatures between 37 °C and 45 °C its size ranges from 0.9 µm to 3.0 µm (Coram & Rawlings, 2002). Several other species can oxidize iron (II) ions and RISC. *Acidiferrobacter* sp. SP3/III (DSM 27195) is an obligated acidophile, Gram-negative mesophilic iron/sulfur oxidizer bacterium, that grows chemolithoautotrophically (Issotta et al., 2018). It was isolated from AMD in Cartagena (Murcia, Spain) (Mitchell et al., 2004).

## 2.4 Biofilms in acidophiles.

Biofilms (BF) are communities of microorganisms embedded in a self-produced matrix of extracellular polymeric substances (EPS), which fills in the interface between the mineral surface and cells, constituting a space for extracellular chemical reactions to occur, making EPS essential constituents for its functionality. BF lifestyle encompass attachment to a solid surface, establishment, maturation, and further cell dissemination (Zhang et al., 2016). BF have emergent properties that are not present in free-living cells, such as: enhanced horizontal gene transfer, cooperation or antagonist interactions between members, resource capture, and an enhanced tolerance and resistance (e.g., resistance to damage caused by reactive oxygen species (ROS), among others. BF formation is regulated by diverse factors, such as environmental signals, and cell-to-cell communication systems (Ng & Bassler, 2009). BF on MS usually form as monolayers in laboratory conditions (Harneit et al., 2006). The processes occurring at bacterial-mineral

interfaces that facilitate leaching are still largely unknown and is it still unclear whether new colonizers benefit form previously existing BF or use them as a signal to attach to rock surfaces, therefore interactions between leaching organisms have been studied aiming to develop countermeasures for AMD and to optimize bioleaching in heaps (Bellenberg et al., 2014).

EPS consists of a highly hydrated matrix consisting of polysaccharides, proteins, lipids, extracellular DNA (eDNA) (Flemming & Wingender, 2010). In some acidophiles grown on pyrite, such as *L. ferrooxidans$^T$* EPS contains neutral sugars, glucuronic acid and complexed iron (III) ions, where the last two components are key to initial attachment to mineral surfaces, due to a net positive charge allowing attachment by electrostatic interactions (Sand & Gehrke, 2006; Zhang et al, 2016). The degree of cell attachment and the amount of complexed iron (III) ions has been positively correlated with bioleaching rates (Sand et al., 2001), highlighting the importance of BF formation as an indicator of bioleaching efficiency. EPS amounts and composition are influenced by the substrate used for growth and can affect the leaching capacity. In leaching bacteria, cell attachment and EPS production results in anode and cathode fixation, charging the pyrite surface and producing metal dissolution (Rohwerder et al., 2003).

**2.5 Quorum Sensing.**

Quorum sensing (QS) constitutes a bacterial cell-cell communication system that controls behaviors in response to changes in cell density. Communication occurs through signal molecules denominated autoinducers (AI). In prokaryotes there are several families of AIs, responsible of regulating a variety of behaviors (Wang et al.,

2004). In Gram-negative bacteria the AI-1 QS system is mainly responsible for intraspecies communication, its AI molecules, denominated N-acyl-homoserine lactones (HSL). These differ from one another on: the length of the acyl-chain (ranging from 4 to 18 carbon atoms), C3 oxidation and saturation of the acyl chain (Watson et al, 2002). The AI-1 QS systems in Gram-negative bacteria is composed of four elements: HSL molecules, an HSL synthase (member of the protein family I), a transcriptional regulator (member of the protein family R) and a *cis* DNA palindromic sequence. Firstly, described in *Vibrio fischeri*, whose luciferase *lux* operon regulates the expression of *luxICDABE* through the proteins LuxI (an HSL synthase), LuxR a cytoplasmatic receptor for HSL and a transcriptional activator (Ng & Bassler, 2009). In leaching bacteria, a functional AI-1 QS system has been described. *Acidithiobacillus ferrooxidans* ATCC 23270[T] possess a *lux*-like QS system denominated *afeI/afeR* (Farah et al., 2005). External addition of a mixture of HSLs positively modulates EPS production and BF formation (González et al, 2012). Similar results were obtained in *Acidiferrobacter* sp. SP3/III and *L. ferrooxidans*[T], in experiments of external addition of HSLs, were enhanced BF formation and attachment was observed in axenic cultures (Bellenberg et al., 2014), while mutualistic inhibition of pyrite dissolution was observed in binary cultures. Also, acidophiles such as *Acidiferrobacter* sp. SP3/III *and Acidithiobacillus thiooxidans*[T] synthesize C10-HSL, C12-HSL, O-C12-HSL, C14-HSL, O-C14-HSL and C16-HSL (Bellenberg et al., 2014), and *Acidiferrobacter* sp. SP3/III possess a *luxR* family transcriptional regulator (Issotta et al., 2018). In addition, *L. ferriphilum*[T] possess *luxR* protein-encoding genes, although at low RNA transcript or protein levels (Christel et al., 2018). These findings support the existence of communication between different species during mineral colonization.

Another family of signal molecules is the diffusible soluble factor (DSF), this QS system found initially in *Xanthomonas campestris* pv. *campestris* (Xcc) (Barber et al., 1997) and previously known as an inter-kingdom communication system between eukaryotes and prokaryotes, is known for its BF dispersing action (Ryan & Dow, 2011). The *rpf* (regulation of pathogenicity) gene cluster is responsible for DSF (*cis*-11-methyl-dodecenoic acid). In *Burkholderia cenopacia* it is responsible for *cis*-2-dodecenoic acid, or *Burkholderia* DSF (BDSF) production, this cluster and its homologs in different species, are responsible for sensing DSF molecules and response. A complete *rpf* cluster has been recently found to be expressed in *L. ferriphilum*[T] (Christel et al., 2018), while part of this cluster excluding RpfF (DSF synthase) has been found in *Acidithiobacillus caldus*[T] DSM 8584 and *Sulfobacillus thermosulfidooxidan*s[T] DSM 9293 (Bellenberg et al., 2018). External addition of synthetic DSF or BDSF molecules to cultures of *L. ferriphilum*[T] and *S. thermosulfidooxidans*[T] produced BF dispersal and prevented oxidation of soluble iron (II) ions and tetrathionate in axenic and mixed cultures of these species, grown in soluble media or in chalcopyrite. However, a recolonization phenotype in of *L. ferriphilum*[T] and *S. thermosulfidooxidans*[T] was observed in chalcopyrite 24 h post addition of these molecules (Bellenberg et al., 2018).

**2.6 Image analysis and colony identification.**

The characterization of sub-populations in mixed cell communities regarding cell identification, at least at the species level, and the quantification of the population for a given species, is feasible by different methodologies. Flow cytometry, qPCR and epifluorescence microscopy (EFM) are commonly employed techniques. Although techniques for cell tracing and labelling eukaryotic cell lines exist, and are widely used, in

acidophilic microorganisms their use present increased difficulty. There is a lack of simple tools and techniques to genetically modify acidophiles (Inaba et al., 2018). Techniques such as qPCR require DNA extraction and, for MS attached cells, their necessary cell detachment step introduces bias, as it has been shown that MS attached cells are extremely recalcitrant to detachment methods. Additionally, indirect methods for determining BF formation, such as planktonic cell counting do not allow BF growth assessment, and methods such as qPCR have issues related to the quality of DNA-extracted from MS attached cells (Bellenberg et al., 2018).

Accurate high-throughput BF analysis and quantification requires a direct non-invasive method, such as automatic image analysis, for which a broad range of software are available. EFM is currently used for biofilm studies and quantitative assessment of BF development on MS. Microbial attachment to pyrite does not occur randomly and evenly distributed (Bellenberg et al., 2018), causing heterogeneous cell attachment patterns on its surface. As a result, in fine-ground mineral particles studies, a large number of grain particles must be analyzed, for example taking a composite or random pictures, Figure 1, in order to obtain a representative percent of superficial mineral area, and to decrease the coefficient of variation in the measurements, for achieving a quantitative assessment of BF formation.

Cell attachment patterns have been recognized through the use of convolutional neural networks allowing species specific identification for *A. caldus$^T$*, *L. ferriphilum$^T$* and *S. thermosulfidooxidans$^T$*, on chalcopyrite surfaces, by using the same cell stain for all species. This methodology requires a training set of >600 images (Bellenberg et al.,

2018), in order to be able to recognize distinct cells in a multi-species BF. Pattern recognition is necessary as the studied cells do not have distinguishable morphologic features for allowing a simple identification of species within mixed BF cultures. A comparison of different image analysis software available has not been done for BFs of acidophiles.
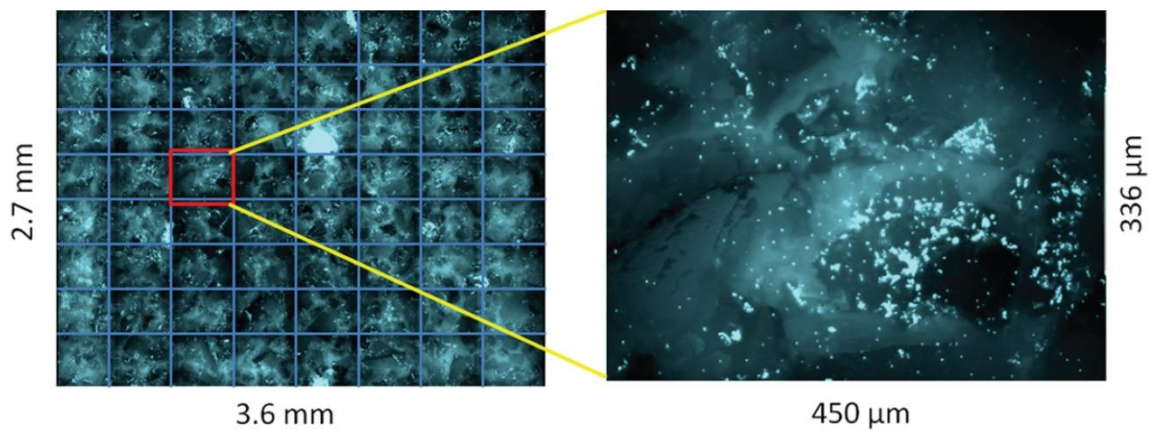


**Figure 1. Experimental setup for automated imaging. Image modified from Bellenberg et al., 2018.** Stack images taken using EFM, automated image acquisition was performed using an AxioImager M2m (Zeiss) fluorescence microscope equipped with a motorized microscopy stage (IM SCAN 130 x 85, DC 1 mm; Märzhäuser Wetzlar) and a AxioCam MRm camera. Images were acquired using a Zeiss filter set 09 for DAPI-stained samples or bright-field mode with background.

**2.7 Staining of acidophilic microorganisms.**

A variety of techniques and dyes have been used for staining acidophilic organisms, the most commonly used are DAPI and Syto 9, these stains are used for binding nucleic acids and therefore are efficient but not species specific in their action. Lectins are

proteins or glycoproteins that bind non-destructively and reversibly to carbohydrates. Lectins such as Concanavalin A (ConA) that binds to glucose and mannose residues (Goldstein et al., 1965), have been used for staining of acidophilic archaeal and bacterial BF for *in situ* studies (Zhang et al., 2015), however EPS are composed of a complex mixture of macromolecules, with a similar composition between species (Zhang et al., 2015), that changes throughout BF maturation, and is also depending on the growth conditions and electron donors (Gherke, 1998; Li & Sand, 2017), therefore lectins are not suited for species specific recognition.

Fei Mao (FM) dyes are amphiphilic fluorochromes, whose fluorescence significantly increase in hydrophobic environments. They have high affinity for lipid-rich domains and consequently have been used to study endocytosis, vesicle trafficking and organelles in eukaryotic cells (Bolte et al., 2004). Lectins and FM-dyes have been used for staining EPS glycoconjugates and the membrane of the archaeal cells *Sulfolobus metallicus* DSM 6482$^T$ and *Ferroplasma acidiphilum* DSM 28986$^T$, respectively, obtaining clear cell-corresponding signals (Zhang et al., 2015). The lipophilic indocarbocyanine 1,1′-dialkyl 3,3,3′,3′-tetramethylindocarbocyanine (DiIC) is a fluorochrome composed by a polar head and two hydrophobic alkyl chains (Guallapalli et al., 2008), emitting an orange-red fluorescence (Nagy, 2013), and presents a greater lipophilic character than FM-dyes (Wiederschain, 2011). DiIC has been used for tracing in fixed and *in vivo* nervous system, due to its high photostability and low toxicity (Nagy, 2013). It has also been used in eukaryotic microorganisms for membrane vesicle tracing (Nicola et al., 2009). So far only FM dyes have been used for staining of acidophilic bacteria (Zhang et al., 2015), while carbocyanines have not been yet used in this context. Their use in acidophilic

Gram-negative bacteria could allow for staining of the cell membrane, as the hydrophobic alkyl chains remain embedded in the membrane, parallel to the phospholipids. As this stain is passed between generations to daughter cells but not between adjacent cells, it allows the tracking a subpopulation of cells without transforming or damaging their DNA. Currently no studies have been made on a species-specific cell recognition and quantification through membrane labeling. A protocol for species-specific labeling based on a combination of membrane staining and nucleic acid counter-staining would allow quantification in mixed cultures.

In this work a protocol for staining BF of the acidophilic bacteria *L. ferrooxidans*[T] and *Acidiferrobacter* sp. SP3/III with DiIC was optimized. EFM photos of *L. ferrooxidans*[T] stained with 2 different cell dyes, were acquired, and analyzed using 3 image analysis software packages: Fiji, Zen 3.0 Image analysis module and a custom script, written in Python 3.0. Fiji (Fiji is just ImageJ), is an open-source image processing software, that supports the use of diverse plugins. Zen 3.0 is a software developed by Zeiss that allows the purchase of modules for image analysis and processing. While the script written in Python 3.0 has been custom-made for pyrite and cell recognition and quantification. The image analysis software evaluated for this work comprise three common main steps: object delineation, signal to background differentiation through a threshold value, and quantification of the desired signals. Differences between these software quantification results arise from the chosen parameters, and additional options offered by each software. Results were compared, in order to evaluate each program. Finally, the effect over BF formation and cell dispersion on the species *L. ferrooxidans*[T] and *L. ferriphilum*[T] caused by external addition of the QS molecules N-dodecanoyl-homoserine lactone ($C_{12}$-

HSL), N-3-dodecanoyl-homoserine lactone (O-C$_{12}$-HSL), N-tetradecanoyl-homoserine lactone (C$_{14}$-HSL), as well as N-3-tetradecanoyl-homoserine lactone (O-C$_{14}$-HSL) of the HSL family was quantified by using the custom script. Additionally, *cis*-11-methyl-dodecenoic acid (DSF) and *cis*-2-dodecenoic acid (BDSF) belonging to the DSF family were added and changes in attachment or dispersion in *L. ferrooxidans*[T] and *L. ferriphilum*[T] were quantified by using the custom script.

## 3 Hypothesis.

Comprehensive BF analysis methodologies require development of robust BF analysis tools and the comparison of different cell dyes as well as development of custom-made software for high-capacity image analysis.

## 4 General Objectives.

-To further advance in the development of BF analysis methodologies based on image recognition through custom-made software.

- To develop a protocol for double staining of leaching bacteria by using membrane staining and nucleic acid staining.

### 4.1. Specific Objectives.

-To optimize a protocol for membrane cell staining of axenic cultures of the leaching species *Acidiferrobacter* sp. SP3/III, and *L. ferrooxidans*[T.]

-To quantify BF formation in axenic cultures of *L. ferrooxidans*[T] and *L. ferriphilum*[T] and to assess if quantified membrane stain signal in *L. ferrooxidans*[T] is positively related to the degree of mineral attached cells.

-To evaluate different image analysis software for colony quantification.

-To quantify BF attachment and dispersion of *L. ferrooxidans*[T] and *L. ferriphilum*[T] exposed to DSF and HSL signaling molecules.

## 5 Materials and Methods.

### 5.1 Materials.

### 5.1.1 Equipment.

- DAIHAN SCIENTIFIC® WIS-30 Shaking incubator.

- CRYSTE® multi centrifuge VARISPIN 12.

- Labnet® SPECTRAFUGE centrifuge 24D.

- ZEISS epifluorescence microscope AXIO OBSERVER Z1/7.

- Motic® Phase-contrast microscope BA310E.

- Hanna® HI 6622 pH meter + electrode HI3310B.

- Vision Scientific vortex KMC-1300V.

- MRC Ltd. Analytical balance ASB-220-C2.

- Thoma® Neubauer improved chamber.

- Stove MEMMERT®.


### 5.1.2 Laboratory Equipment.

- Falcon tubes 15 and 50 mL.

- Sterilized glass Schott bottles 50, 300 and 1000 mL.

- Eppendorf tubes 600 µL, 1500 µL and 2000 µL.

- Micropipetes 1000 µL, 200 µL, 100 µL, 20 µL, 2 µL.

- Microscopy slides.

- Microscopy cover slips.


### 5.1.3 Reagents used for bacterial cultures.

- Mackintosh (MAC) medium, (Mackintosh, 1978). **Solution A**: $(NH_4)_2SO_4$ [1 mM], $H_2SO_4$ [9,8 mM]. **Solution B**: $KH_2PO_4$ [0,2 mM]. **Solution C**: $MgCl_2$ x 6 H2O [0,1

mM], $CaCl_2 \times 2\ H_2O$ [1 mM]. **Trace elements**: $MnCl_2$ x $4H_2O$ [1,19 x 10-5 mM], $ZnCl_2$ [1,02 x$10^{-5}$ mM], $CoCl_2 \times H_2O$ [5,04 $\times$ $10^{-5}$ mM], $H_3BO_3$ [5,01x$10^{-5}$ mM], $Na_2MoO_4 \times 2\ H2O$ [5,0 $\times$ $10^{-6}$ mM], $CuCl_2 \times 2\ H_2O$ [4,99 $\times$ $10^{-6}$ mM]. *Every reagent was acquired from MERCK®

- $FeSO_4 \times 7\ H_2O$ [4 g/L], soluble iron (III), MERCK®.

- $K_2S_4O_6$ [5 g/L] , MERCK®.

- N-dodecanoyl-homoserine lactone (C12-HSL), 1 μM in DMSO, Chemodex.

- N-3-dodecanoyl-homoserine lactone (O-C12-HSL), 1 μM in DMSO, Chemodex.

- N-tetradecanoyl-homoserine lactone (C14-HSL), 1 μM in DMSO, Chemodex.

- N-3-tetradecanoyl-homoserine lactone (O-C14-HSL), 1 μM in DMSO, Chemodex.

- *Cis*-11-methyl-dodecenoic acid (DSF), 5 μM in DMSO, Caymanchem.

- *Cis*-2-dodecenoic acid (BDSF), 5 μM in DMSO, Caymanchem.

### 5.1.4 Dyes.

Nucleic acids stains:

- DAPI (4',6-Diamidino-2-phenylindole, Dihydrochloride), Invitrogen™.

Membrane stains, these are long chain fluorescent carbocyanines whose acyl chains are imbedded in the bilayer parallel to the phospholipid acyl chains, while their chromophore is parallel to the cell's surface (Axelrod, 1979). The dyes from the Thermo Fisher Lipophilic Tracer Sampler kit, Invitrogen™ were used:

a. 3,3'-dioctadecyl-5,5'di(4-sulfophenyl) oxacarbocyanine, sodium salt ('DiO'; SPDiOC18(3)).

b. 1,1'-Dioctadecyl-3,3,3',3'-Tetramethylindocarbocyanine Perchlorate ('DiIC'; DiIC18(3)).

**5.1.5 Bacterial Strains.**

*Acidiferrobacter* sp. SP3/III DSM 27195

*L. ferrooxidans* DSM 2705[T]

*L. ferriphilum* DSM 14647[T]

## 5.2 Methods

**5.2.1 Culture Medium.**

$2.5{\times}10^7$ cells/mL of *L. ferrooxidans*[T] *or Acidiferrobacter* sp. SP3/III were cultivated at 30°C with 100 rpm agitation in MAC medium at pH 1.6, supplemented with 71.6 mM (4 g/L) or 107.4 mM (6 g/L) iron (II), supplied as $FeSO_4 \times 7\ H_2O$ for *Acidiferrobacter* sp. SP3/III (Issotta et al., 2018), or *L. ferrooxidans*[T] (Bellenberg et al., 2014), respectively. *L. ferriphilum*[T] inoculum was grown at 37 °C.

For growth on pyrite, the iron (II) was replaced with either 0.5 % or 2 % w/v Chilean pyrite with a medium size between 50-100 μm for membrane cell tracing and external addition of QS molecules experiments, respectively.

Volumes of 250 mL in 500 mL Erlenmeyer flasks and 20 mL in 50 mL Erlenmeyer flasks were used for growth of the inocula and for performing experiments, respectively. Cell density was determined, as described in 5.2.2. Pyrite and supernatant samples were taken as shown in Table II, pyrite samples were stored at -20 °C for later EFM visualization.

**Table I. Summary of culture media and energy source used for each strain.**

| Bacteria | Medium | Energy Source |
|---|---|---|
| *Acidiferrobacter* sp. SP3/III | MAC pH 1.6 | Iron (II) 4 g/L |
| | MAC pH 2 | Pyrite 2 % w/v |
| *L. ferrooxidans*[T] | MAC pH 1.6 | Iron (II) 6 g/L |
| | MAC pH 1.6 | Pyrite 0.5 % w/v |
| | MAC pH 2 | Pyrite 2 % w/v |
| *L. ferriphilum*[T] | MAC pH 1.6 | Pyrite 0.5 % w/v |

### 5.2.2 Planktonic cells quantification.

Bacterial cell density was determined through cell counting using a Neubauer chamber improved Thoma® (depth: 0.02 mm, area:0.0025 μm$^2$) and a Phase-contrast Microscope Motic BA310E with 400x magnification.

### 5.2.3 Cell harvesting.

Bacterial cells were harvested from iron (II) and pyrite cultures by centrifugation using a 16R MEGAFUGE® at 10,000 g for 15 min at room temperature. The supernatant was

then discarded, and the pellet re-suspended in 2 mL MAC medium, after another 10 min centrifugation at 10,000 × g the supernatant was again discarded, and the pellet re-suspended in 500 μL MAC medium pH 5.4. Subsequently, bacteria were counted to verify that at least a total amount of $10^{10}$ cells remained.

### 5.2.4 Cell staining.

$10^{10}$ cells were washed and 500 μL MAC medium pH 5.4 was added. Cells were stained using a Lipophilic Tracers Sampler kit from Invitrogen™. For staining of the bacterial membrane, the tracers 3,3'-dioctadecyl-5,5'di(4-sulfophenyl) oxacarbocyanine, salt (DiO) at 50 μg/mL, and 1,1'-Dioctadecyl-3,3,3' ,3'-Tetramethylindocarbocyanine Perchlorate (DiIC) at 25 μg/mL were used.

Cells were incubated at room temperature, in darkness, and with medium agitation using a vortex for 2 h. Stained cells were then inoculated in 50 mL flasks filled with 20 mL MAC medium at pH 2 and 2% w/v pyrite. After this step, cell density was determined according to 5.2.2, and the cultures were incubated as described in 5.2.1.

Before microscopy experiments, pyrite grains with attached BFs were washed thrice with filtered water (0,22 μm, Millipore®) and dyed in 600 μL reaction tubes with DAPI 300 nM from Invitrogen™ for DNA staining. The sample was incubated for 20 min in darkness and the DAPI excess was discarded. Lastly, the sample was mounted in a microscope slide and the antifading Citifluor® AF2 mounting medium was added, in order to prolong the durability of the stain.

**5.2.5 Attachment and dispersion assays using HSL and DSF molecules.**

For attachment assays *L. ferrooxidans*[T] and *L. ferriphilum*[T] were grown on pyrite for 2 weeks. Cells were inoculated at a density of $5 \times 10^7$ cells/mL on MAC pH 1.6, with 0.5 % w/v pyrite as electrons source. Planktonic cells were centrifuged as described in 5.2.3 and inoculated in pyrite 0.5 % w/v. Simultaneously HSL or DSF molecules were added. HSLs were added at a concentration of 1 µM (in mixtures of $C_{12}$-HSL and O-$C_{12}$-HSL, as well as $C_{14}$-HSL and O-$C_{14}$-HSL, 0.5 µM of each was added). DSF molecules *cis*-11-methyl-dodecenoic acid (DSF) and *cis*-2-dodecenoic acid (BDSF) were added at 5 µM. Samples were extracted as indicated in Table II. As a solvent control, DMSO 0.1 % w/v was added, while control cultures had no additions.

For dispersion assays *L. ferrooxidans*[T] and *L. ferriphilum*[T] were grown on pyrite for 3 days in 20 mL MAC pH 1.6. Pyrite with attached cells was washed, placed in a new flask and refilled with 20 mL of fresh MAC medium. Simultaneously HSL or DSF molecules were added at the aforementioned concentrations. Samples were taken as indicated in Table II. Controls with DMSO and without additions were also performed as indicated previously.

**Table II. Samples and pictures taken for each experiment of external addition of signaling molecules.**

| Species and external molecule addition | Assay | Samples taken (h) | Photos taken for each sample |
|---|---|---|---|
| *L. ferriphilum* DSF | Attachment | 4, 22, 46, 100, 214 and 310 | 3 |
| *L. ferriphilum* DSF | Dispersion | 18 and 310 | 3 |
| *L. ferriphilum* HSL | Attachment | 22 | 13 |
| *L. ferriphilum* HSL | Dispersion | 22 | 13 |
| *L. ferrooxidans* HSL | Attachment | 70 | 13 |
| *L. ferrooxidans* HSL | Dispersion | 48 | 13 |

**5.2.6 Epifluorescence microscopy.**

BF formation on pyrite grains was visualized with an EFM AXIO OBSERVER Zeiss® Z1/7 using equipped with objectives 20x (N.A. 0.35) and 40x (N.A 0.75). Red, green and blue filters with emission and absorption wave lengths of Ex/Em i) DilC: 538-562/570-640 ii) DiO: 450-490/500-550 iii) DAPI: 335-383/420-470 were used Photos were taken using 40x objective Zeiss® Zen Pro version 2.3, with an image size of 247.10 μm × 184.79 μm per image. Photos were taken using a Z-stack module, with a separation of 0.5 μm, to take multiple pictures of the same sample a motorized Scanning Stage SCAN IM 130 x 100 (Zeiss® Axio Observer) was used. Additionally, to the use of the Z-stack option, the tiles option was used for taking some pictures, for these 16 pictures each with a size of 247.10 μm × 184.79 μm were taken in an arrangement of 4×4. Images were reconstructed using extended depth focus (EDF) module that allows an elongated focal point. EDF processing was done using Zeiss® Zen Pro version 3.0 using the contrast option. Projections were exported as TIFF files.


**5.2.7 Image analysis.**

The Image analysis Software compared were:


Script: The analysis of the images was done using a script kindly provided by Dr. Timothy James Rudge and Isaac Nuñez from the Biological and Medical Engineering Institute UC. Images in *.tiff format were quantified by an automatic script developed in Python 3.0. Images were exported in the channels: DilC, DAPI, brightfield, shift-pixel and composite. Using the automated script, the channels DilC and DAPI were filtered, through the function: (im data = im data['R'], im data['G'], im data['B'], im

data['NormSum'] = get im data (fnames) im data ['name'] = fnames CHANNELS=['R','G','B']). A threshold was defined to identify the colonies (threshold[im num] = 0.39,sigma lim[im num] = [2,14]) and a radius was determined (col values = np.zeros ((A.shape[0], A.shape[1]+2)) col values[:,0:3] = A radii = ((2)**(1/2))*col values[:,2]col values[:,3= radii). The images were normalized via a sigma filter (im num = filter sigma [im num] = 0.5 sImS[im num],sImSall[im num] = smooth data (im data, filter sigma [im num], im num). Finally the area corresponding to the pyrite grains was identified using the bright field image (bf thresh = 3.0 bf cols["bf threshold"]= bf thresh bin bf = binary image(sImSall [im num], bf thresh).Colonies were selected form the DAPI and DilC channel and later the correlation was made in base to the membrane and DAPI signals.

Fiji: The images in *.tiff format were quantified using Fiji. For this, black and white images were used. The threshold for cell counting was set manually, carefully avoiding by sight the consideration of noise in the colony counting. All cells in the field of view were counted, as it was not possible (without using additional software packages) to identify pyrite grains and filter cell signal outside them.

Zen 3.0 Image analysis module: Zen 3.0 is a private software developed by Zeiss that allows the purchase of modules made for specifics tasks. The image analysis module allows a variety of analysis for microscopy images. Seven steps for image analysis with Zen pro 3.0 can be used. 1.Classes: Allows to select the desired channels to analyze and their hierarchy, here either DAPI or DilC was selected. 2. Frame: This step allows to select a region of interest (ROI), here the whole image was selected. 3 Interactive segmentation: Allows the smoothing of the image (value selected was 141), setting a

threshold (value selected was -125) selecting a minimum area for the analyzed spots (value selected was 1), other options are available, but they were left as the original default settings of the software. 4. Region Filter: Allows the selection and setting of a variety of filters, in this work the filters selected were: radius, Intensity minimum of channel bright, Intensity maximum of channel bright, and Intensity maximum of channel DAPI. This setting allows for filtering of signal spots outside pyrite grains. Additionally, thresholds for these options were adapted for each image, using the interactive option offered by Zen 3.0, allowing to include signal spots with varying brightness intensity, while at the same time excluding bright spots too big to represent a colony. 5. Interactive segmentation: Allows to manually select areas to be analyzed, this option was not used. 6. Features: Allows to select the information obtained from the image. Data such as area of the colonies, ID, and radius was selected. 7. Results preview: Allows to visualize a prior result of the analysis, and to confirm if this has been performed as the user specified. Finally, the information obtained was exported as a .csv file and colonies counted using the ID for each image dataset.

## 6. Results.

### 6.1 Cell staining.

The use of the membrane stains DiIC and DiO for tracing *L. ferrooxidans*[T] and *Acidiferrobacter sp.* SP3/III BFs was evaluated. For this, images of BFs stained with either DiIC or DiO, and counter-stained with DAPI were taken using EFM and the tiles option of Zen pro 2.3. The performance of the membrane staining was evaluated based on the diameter of the observed spots. It was observed that DiO produced signal spots with a greater size compared to DAPI signal spots, and even bigger spots than what is expected for bacterial cells, therefore further experiments were performed using DiIC stain, Figure 2.
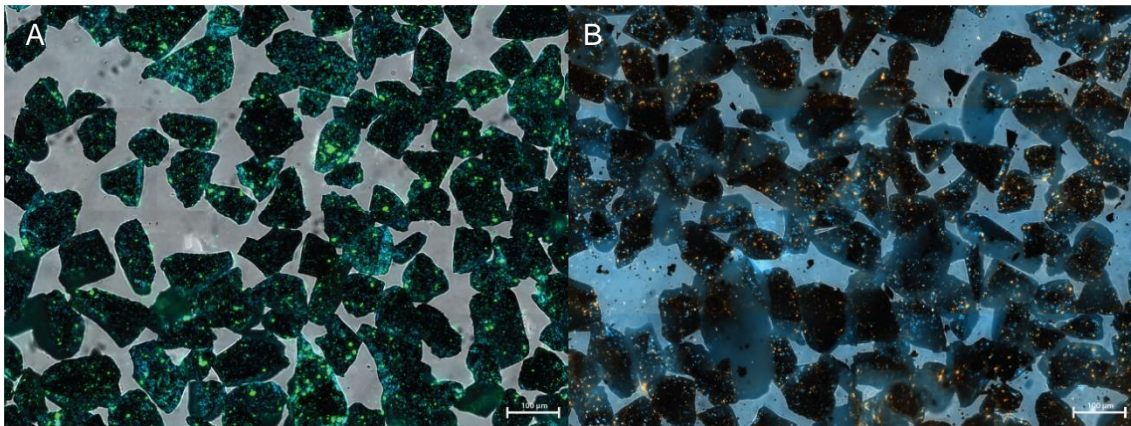


**Figure 2. Comparison of BF patterns by *Acidiferrobacter* sp. SP3/III, pre-stained with membrane dyes.** Attached *Acidiferrobacter* sp. SP3/III to the surface of pyrite grains after 24 h of BF formation are shown. Images were taken using Z-stack and tiles option. A. DiO pre-stained cells, counter-stained with DAPI B. DiIC pre-stained cells counter-stained with DAPI. Size bars indicates 100 µm.

Attachment to pyrite of *L. ferrooxidans*[T] and *Acidiferrobacter* sp*.* SP3/III was confirmed through EFM images of DiIC pre-stained cells and DAPI stained cells, after 24 h of incubation in pyrite. We observed the presence of BFs on pyrite when DiIC was used, the size, localization and frequency of the DiIC signal spots with respect to DAPI signal spots was observed, Figure 3.
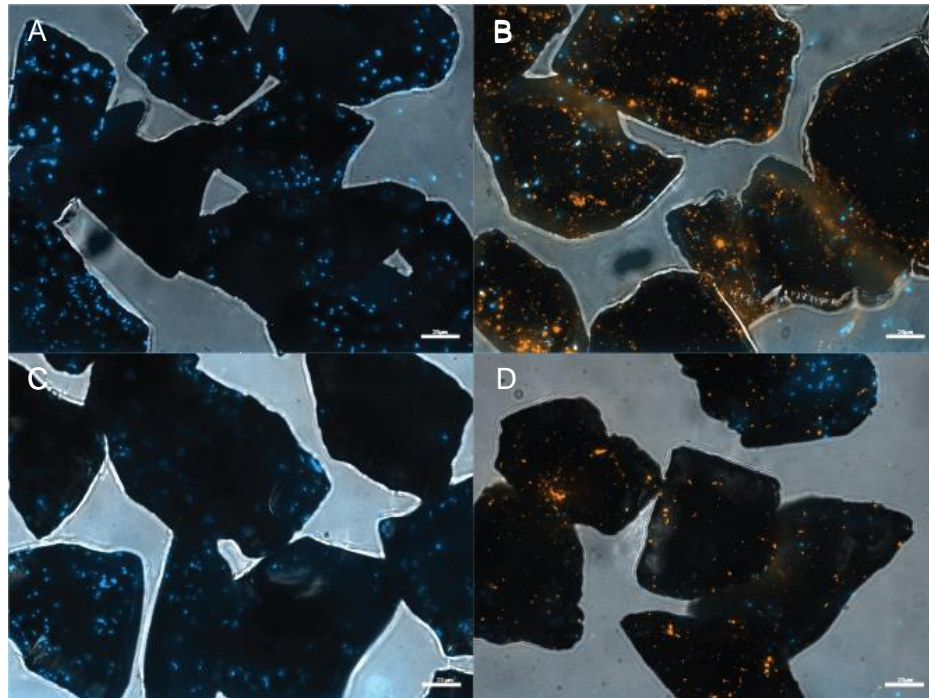


**Figure 3. Comparison of the localization and sizes of DiIC signal spots respect to DAPI signal spots.** Stack images taken using EFM, image acquisition performed using a fluorescence microscope equipped with a scanning stage SCAN IM 130 x 100 (Zeiss® Axio Observer). Attached leaching bacteria to pyrite grains after 24 h of BF formation are shown. A. *L. ferrooxidans*[T] stained with DAPI B*. L. ferrooxidans*[T] pre-stained with DiIC, and counter-stained with DAPI C. *Acidiferrobacter* sp. SP3/III stained with DAPI D. *Acidiferrobacter* sp. SP3/III pre-stained with DiIC and counter-stained with DAPI. Size bars indicates 20 μm.

## 6.2 Influence of lipophilic stain over bacterial attachment to pyrite surfaces and comparison between image analysis software.

To evaluate the effect of membrane pre-staining with DiIC over attachment of *L. ferrooxidans*[T] cells to the surface of pyrite grains in time, media samples and pyrite grains were taken at: 24 h, 48 h, 72 h, 96 h and 120 h, to follow planktonic cell density and BF formation, respectively. The growth of the planktonic cell population in cultures inoculated with iron (II) or pyrite was assessed, Figure 4. Similar growth of the planktonic population was observed between unstained and DiIC pre-stained cultures, with no significant differences in planktonic cell density between unstained and pre-stained cells.

However, cultures inoculated with cells grown on pyrite had a greater density of the planktonic cells population compared to iron (II) grown cells, where planktonic cell density for cultures of unstained cells was higher in almost all points compared to stained cells for both inocula.

Samples of *L. ferrooxidans*[T] BFs on pyrite were visualized using EFM, all samples were stained with DAPI before visualization. Images were taken in random locations of the sample. A total of 4 images for each sample, each one composed of Z-stacks of 80 layers of 0.5 μm (with a total span of 40 μm in Z-axis). The quantification of signal spots and calculation of the pyrite covered area in percentage, was made using the custom-made script. Cell counts were normalized by dividing the number of quantified signal spots by the pyrite covered area (in $mm^2$) of each image set.
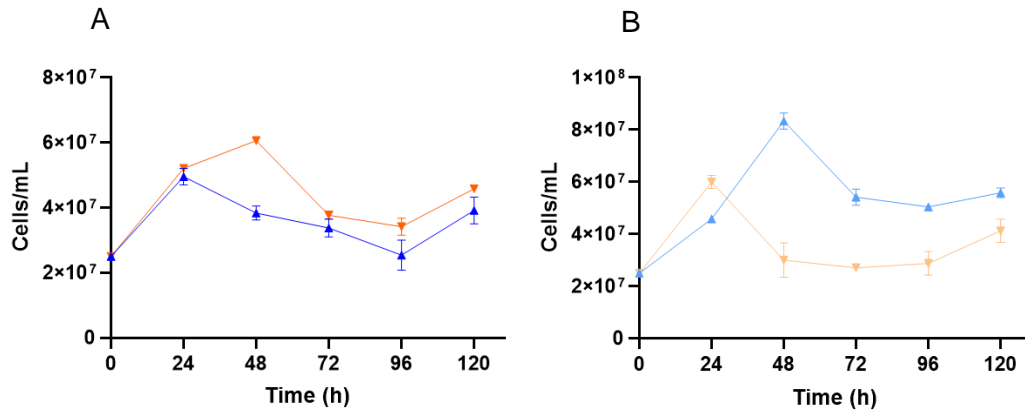
**Figure 4. Comparison of planktonic cell growth for unstained and DilC pre-stained *L. ferrooxidans*[T] cultures. Effect of DilC over planktonic cell growth.** Cell counts were done in triplicate, and replicas for cultures inoculated with cells grown on iron (II) were averaged. A. Cultures inoculated with iron (II) grown cells, unstained or pre-stained with DilC. B. Cultures inoculated with pyrite grown cells, unstained or pre-stained with DilC.

Images of BFs of *L. ferrooxidans*[T] stained with DAPI or pre-stained with DilC were taken, for cultures inoculated with cells grown either on iron (II) (Figure 5) or pyrite (Figure 6). The number of attached cells to the pyrite surface either on DilC pre-stained cultures and cultures stained only with DAPI after sample collection was estimated through the quantification of the DAPI signal spots, although not all signal spots were recognized by the software, therefore absolute quantification was performed, results were relative to one another. Quantification was performed using a custom-made software for analyzing EFM images of BF on pyrite, signal spots on the DAPI channel were quantified and divided by the pyrite area in mm$^2$ covering the image, results are shown in Figure 7 (a) and Figure 8 (a), for iron (II) and pyrite grown cells used as inoculum, respectively.

Cultures pre-stained with the lipophilic stain DiIC were counter-stained with DAPI for comparison. The signal spots on the DAPI channel were quantified, Figure 7 (b) and Figure 8 (b). The signal of the channel DiIC was observed to decline over time, this could happen due to the fact that this stain binds to the cell membrane, and it's expected to be diluted after every cell division, Figure 5 (B, D, F, H, J) and Figure 6 (B, D, F, H, J). DiIC signals spots were quantified for DiIC pre-stained cells grown on iron (II), Figure 7 (C), and for cells grown on pyrite, Figure 8 (C).

Quantification results in the DAPI channel were compared between results obtained for samples of BFs pre-stained with DiIC and BFs stained with DAPI only, this was done by stablishing a ratio between the DAPI signal counts obtained for DAPI stained and pre-stained cultures, Figure 7 (D), and Figure 8 (D). The ratio was used to assess the effect of the membrane stain over cell attachment to the mineral, a ratio of one implies that no changes in attachment occur as a result of pre-staining.
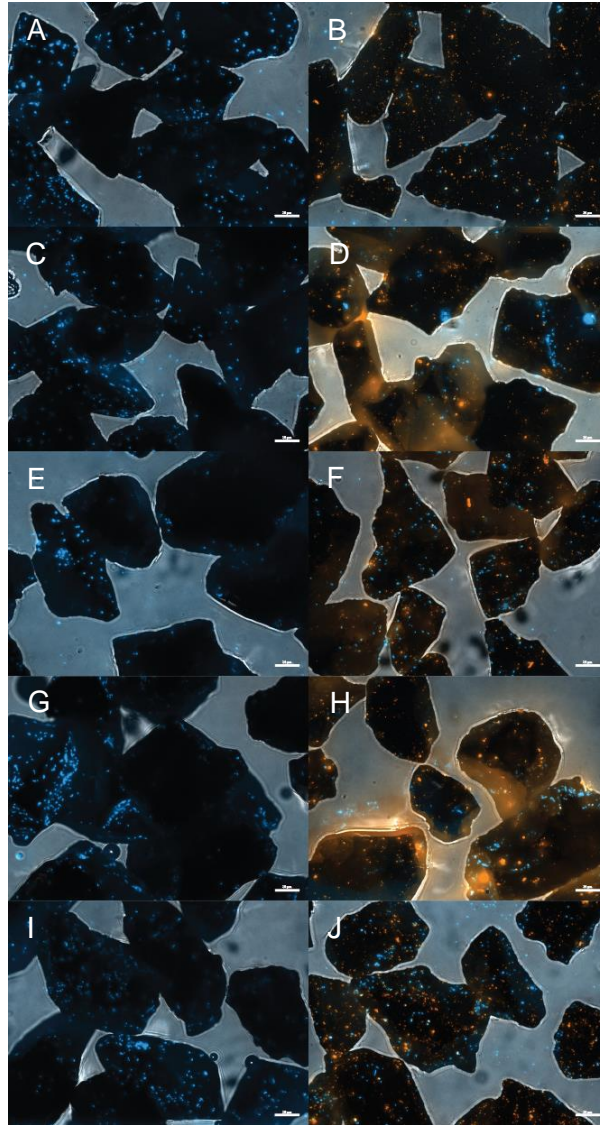
**Figure 5. Examples of quantified images, comparison of DAPI stained cultures (left column) and DilC pre-stained cultures counter-stained with DAPI (right column), for cultures of _L. ferrooxidans<sup>T</sup>_ inoculated with iron (II) grown cells.** Pyrite samples were extracted and imaged after 24 h (A and B), 48 h (C and D), 72 h (E and F), 96 h (G and H) and 120 h (I and J). Size bars indicates 20 μm.
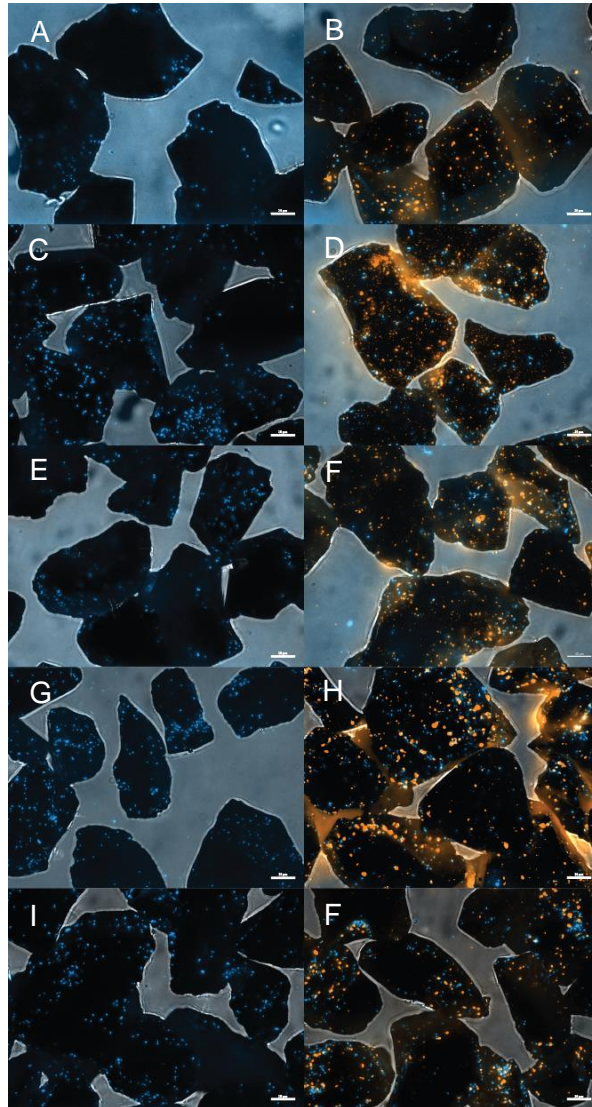
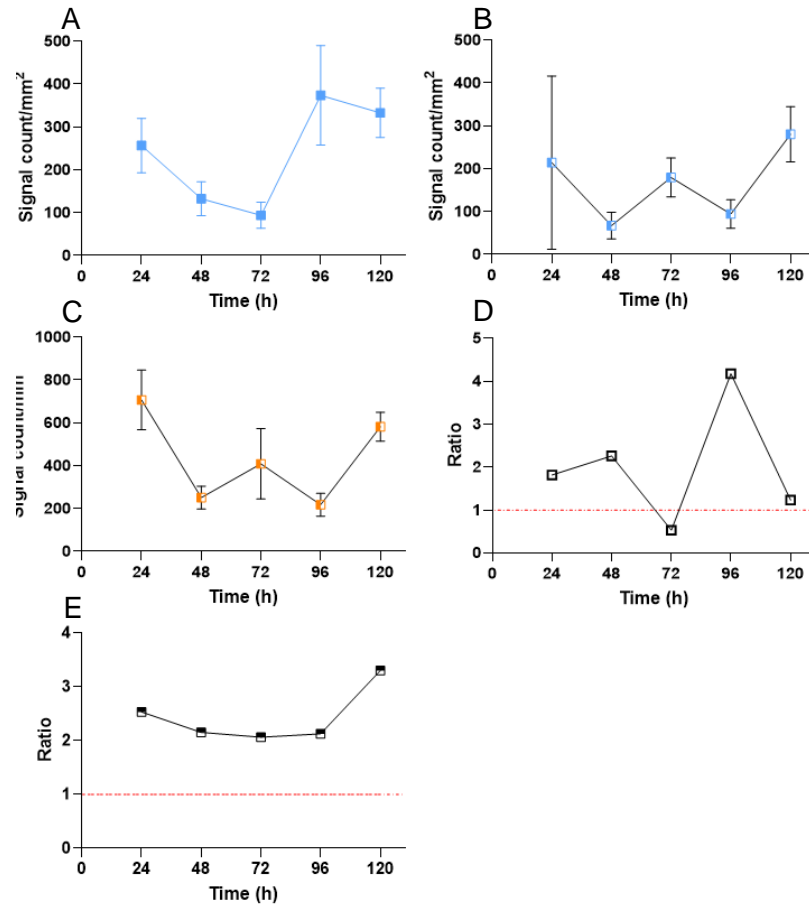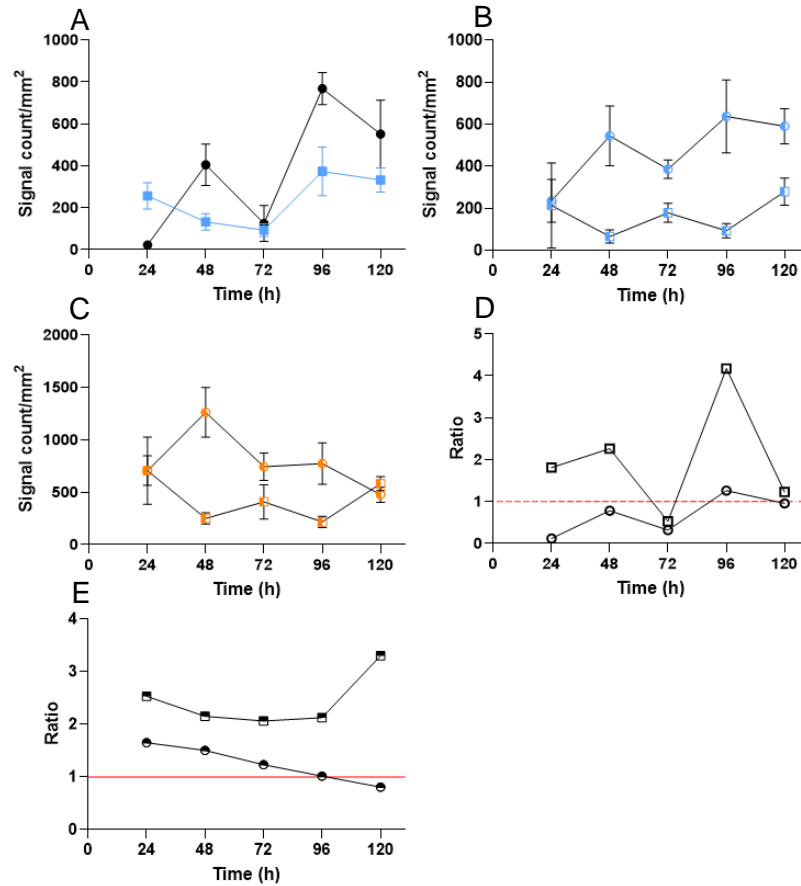**Figure 6. Examples of the quantified images, comparison of DAPI stained cultures (left column) and DilC pre-stained cultures counter-stained with DAPI (right column), for cultures of *L. ferrooxidans*[T] inoculated with pyrite grown cells.** Pyrite samples were extracted and imaged after 24 h (A and B), 48 h (C and D), 72 h (E and F), 96 h (G and H) and 120 h (I and J). Size bars indicates 20 μm.

**Figure 7. Quantification of the signal spots in the channels DAPI and DilC for images of *L. ferrooxidans* BFs on pyrite, inoculum grown on soluble iron (II).** Four images were quantified for each datapoint. A. DAPI stained cells, DAPI channel quantified signal spots per $mm^2$ of pyrite surface. B. DilC pre-stained cells, DAPI channel quantified signal spots per $mm^2$ of pyrite surface. C. DilC pre-stained cells, DiI channel quantified signal spots per $mm^2$ of pyrite surface. D. Ratio between quantified signal spots obtained for DAPI signal between DAPI stained, and DilC pre-stained cells E. Ratio between quantified signal spots made for DilC pre-stained cells for DilC and DAPI channel. Dashed line indicates 1 in y-axis. Quantification was done using custom script.

**Figure 8. Quantification of the signal spots in the channels DAPI and DilC for images of *L. ferrooxidans*[T] BFs on pyrite, inoculum grown pyrite.** Four images were quantified for each datapoint. A. ● DAPI stained cells, DAPI channel quantified signal spots per mm$^2$ of pyrite surface. B. ● DilC pre-stained cells, DAPI channel quantified signal spots per mm$^2$ of pyrite surface. C. ● DilC pre-stained cells, DiI channel quantified signal spots per mm$^2$ of pyrite surface. D. ● Ratio between quantified signal spots obtained for DAPI signal between DAPI stained, and DilC pre-stained cells. E. ● Ratio between quantified signal spots made for DilC pre-stained cells for DilC and DAPI channel. Dashed line indicates 1 in y-axis. Quantification was done using custom script.

Additionally, for BFs pre-stained with DiIC the quantification results obtained for DiIC and DAPI channels were compared. This comparison was done by stablishing a ratio between the DiIC signal counts and DAPI signal counts in every image, Figure 7 (E), and Figure 8 (E). The ratio was used to assess the proportion between signal spots for each dye, a ratio of one indicates that the same number of signal spots is seen in both channels (although this does not mean a colocalization between the signals, as this was not measured), while a ratio above one indicates that more signal spots in the DiIC channel are present than DAPI signal spots, and a ratio below one indicates that more signal spots are quantified in the DAPI channel than on the DiIC channel.

Quantification results obtained via script for images of *L. ferrooxidans*[T] BFs on pyrite, for cultures where cells grown on iron (II) ions were used as inoculum, were compared to cultures where pyrite grown cells were used as inoculum, Figure 8. A greater cell count per unit of pyrite surface area was obtained when pyrite grown cells were used as inoculum. This tendency was observed for most points, independent of the dye used, Figure 8 (A, B and C). The ratio between cell counts obtained for DAPI channel for DAPI stained and DiIC pre-stained cells in cultures with pyrite grown cells used as inoculum, was observed to be closer to one compared to cultures inoculated with iron (II) grown cells, Figure 8 (D). In contrast to cultures with iron (II) grown cells used as an inoculum, more signal spots in the DAPI channel were quantified for DiIC pre-stained cells than for DAPI stained cells, Figure 8 (E). These results indicate that DiIC is viable for tracing of BF development, achieving analogous growth and attachment with DiIC stained cells compared to unstained cells. Moreover, it is useful even under the harsh oxidizing conditions that occur in acidic pH and in the oxidizing surface of pyrite.

Subsequently, the images in the channels DAPI and DiIC were re-quantified using Zen 3.0 equipped with an image analysis module and Fiji, this analysis was performed for cultures inoculated with iron (II) grown cells, Figure 9 and for cultures where pyrite grown cells were used as inoculum, Figure 10. Signal spots quantification results were not divided by the pyrite area visible on the images, as only the custom-made script allows for simultaneous quantification of pyrite coverage of the image and dye signal quantification. Interestingly, it was observed Zen 3.0 was able to recognize the most spots of signal, even though spots outside the grains were filtered. Contrarily, Fiji quantified a similar count of signal spots compared to the custom-script, although this software, when no additional packages are used, does not allow for filtering of the colonies outside the grains.
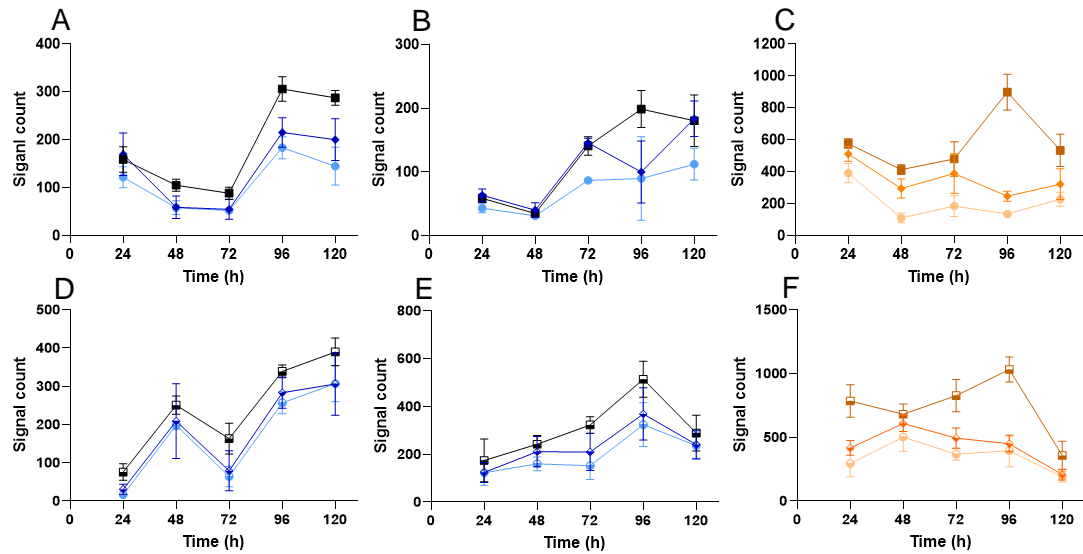
**Figure 9. Comparison of quantification results in the channels DAPI and DiIC obtained using the software Zen 3.0, Fiji and custom-script for images of *L. ferrooxidans* BFs on pyrite. Inoculum grown on soluble iron (II) (upper row) or pyrite (lower row).** Four images were quantified for each datapoint. Images were quantified using Zen 3.0 (squares,■ DAPI and ■ DiIC channels), custom-script (circles, ● DAPI and ● DiIC channels) or Fiji (diamonds,◆ DAPI and ◆ DiIC channels). Fully colored shapes indicate inoculum grown on iron (II) and half colored shapes indicate inoculum grown on pyrite. A and D. DAPI stained cells, DAPI channel quantified signal spots. B and E. DiIC pre-stained cells, DAPI channel quantified signal spots C and F. DiIC pre-stained cells, DiIC channel quantified signal spots.

## 6.3 Effect of external addition of HSL and DSF molecules.

The effect of the external addition of HSLs over dispersion and attachment of *L. ferriphilum*[T] and *L. ferrooxidans*[T] was studied. During dispersion assays, fresh media was added to already pre-colonized pyrite with these species for 72 h. Simultaneously

with the addition of fresh media, HSL molecules (5 µM dissolved in DMSO) were added and pyrite samples were extracted, stained with DAPI and imaged. DMSO addition was used as a solvent control, finding no significant difference to no addition in control cultures, Figure 10. No significant differences in cell dispersion for *L. ferrooxidans*[T] or *L. ferriphilum*[T] were observed, comparing HSLs addition to addition of DMSO or no addition, also a high standard deviation was obtained, for the quantification results, even in control cultures.
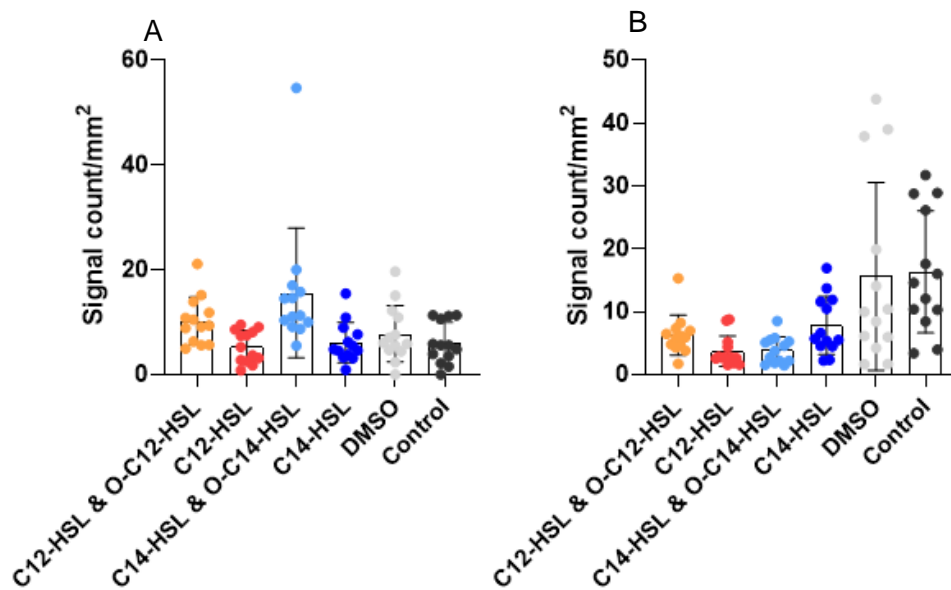


**Figure 10. Quantification of the signal spots in the channel DAPI for images of *L. ferrooxidans*[T] and *L. ferriphilum*[T] BFs on pyrite after HSL addition, dispersion assays.** Inocula was grown for 72 h in pyrite. For each point 13 images were quantified using custom script. DMSO was added as a solvent control, while in control cultures there were no additions. A. *L. ferrooxidans*[T] dispersion assay, pyrite samples were taken after 22 h of HSL and media addition. B. *L. ferriphilum*[T] dispersion assay, pyrite samples were taken after 22 h of HSL and media addition.

In attachment assays, media containing pyrite grown planktonic cells was added to pyrite with a final pyrite concentration of 0.5 % w/v. A significant diminished attachment ($p<0.001$) of *L. ferrooxidans*[T] to pyrite surface was quantified in cultures with addition of mixtures of HSLs (C12-HSL with O-C12-HSL, and C14-HSL with O-C14) in comparison to cultures with DMSO addition, Figure 11 (A). For *L. ferriphilum*[T] cultures, a decrease on cell attachment was observed upon addition of C12-HSL with O-C12-HSL ($p<0.001$), and 3-oxo-C14-HSL ($p<0.002$), while C14-HSL with 3-oxo-C14-HSL ($p<0.033$) had a moderate effect over attachment in comparison to cultures with DMSO addition, Figure 11 (B), however *L. ferriphilum*[T] samples were taken 48 h after pyrite addition, in contrast to *L. ferrooxidans*[T] samples taken after 70 h, and therefore differences in attachment are not comparable between these two species.
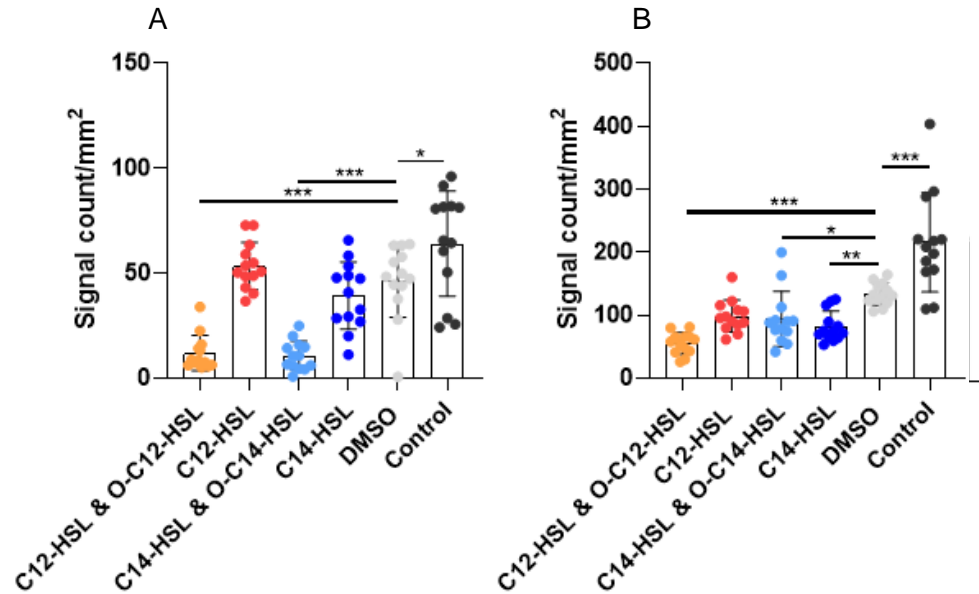
**Figure 11. Quantification of the signal spots in the channel DAPI for images of *L. ferrooxidans*[T] and *L. ferriphilum*[T] planktonic cells on pyrite after HSL addition, attachment assays.** For each point 13 images were quantified using custom script. DMSO was added as a solvent control, while in control cultures there were no additions. A. *L. ferrooxidans*[T] attachment assay, pyrite samples were taken after 70 h incubation. B. *L. ferriphilum*[T] attachment assay, pyrite samples were taken after 48 h incubation.

It is worth noting that significant differences between the control cultures with DMSO addition and no additions were measured for attachment assays in *L. ferrooxidans*[T] ($p<0.033$) and *L. ferriphilum*[T] ($p<0.001$), these differences were not seen in dispersion assays, therefore it is not possible to assert that the addition of DMSO had no effect over the attachment of the cells. Accordingly, the differences in attachment were measured using the solvent control.

The effect of the external addition of DSF molecules over attachment and dispersion of *L. ferriphilum*[T] was also studied, Figure 12. During attachment assays a great variation of the quantified signal was observed, with a spike in cell attachment at 4 h, however differences in attachment ($p < 0.001$) between cultures with DMSO and no addition were measured, and no differences in attachment were quantified as a result of DSF or BDSF addition, in comparison to the solvent control with DMSO, indicating that the measured differences to the control culture with no addition could be explained by the solvent present in the samples. Furthermore, no significant differences in attachment to pyrite or cell dispersion for *L. ferriphilum*[T] as a result of DSF or BDSF addition were measured. It is worth noting that only three images per condition were analyzed, in order to assert the effect of the use of DSF QS molecules over attachment or dispersion of *L. ferriphilum*[T] it becomes necessary to repeat these experiments and to quantify a larger dataset.
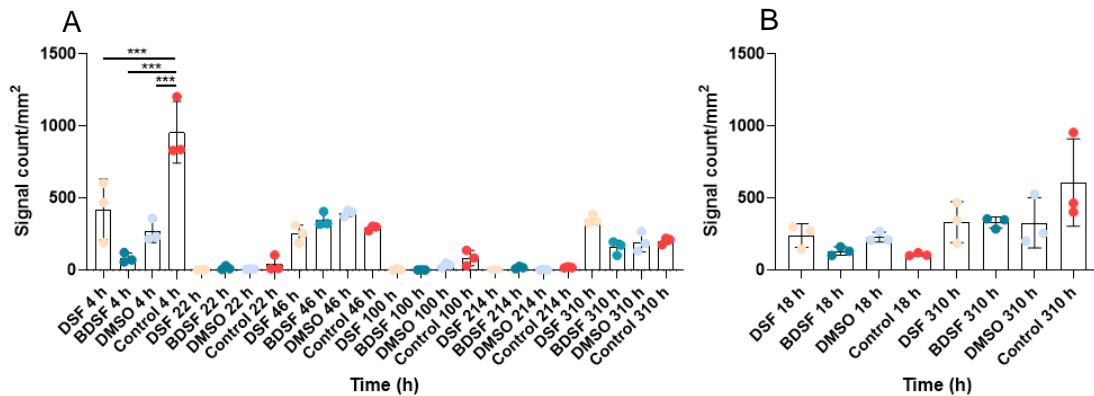


**Figure 12. Quantification of the signal spots in the channel DAPI for images of *L. ferriphilum*[T] BFs on pyrite after DSF or BDSF addition.** For each point 3 images were quantified using custom script. DMSO was added as a solvent control, while in control cultures there were no additions. A. Attachment assay B. Dispersion assay.

## 7 Discussion.

### 7.1 Cell staining.

As DilC stays in the cell membrane and DAPI bind to the DNA in the nucleus, therefore it is possible to have a cell stained simultaneously with both stains. However, unlike DAPI, DilC does not disrupts the normal functioning of the cells and therefore could be suitable for cell tracking purposes. Membrane staining assays suggests that DilC is potentially useful for tracing *L. ferrooxidans*[T] and *Acidiferrobacter* sp. SP3/III BFs development, as the observed signal spots in the DilC channel are of sizes according to what is expected for bacterial cells and big signal spots were uncommon, Figure 2 (B) and Figure 3 (B and D). In contrast DiO produced multiple signal spots on the pyrite surface, with a larger size than what is expected for a colony and a frequency with no apparent relation to the degree of colonization of the pyrite surface, Figure 2 (A). Therefore, DilC was selected for pre-staining assays in *L. ferrooxidans*[T] BFs. DilC pre-stained cultures counter-stained with DAPI showed presence of signal spots in both channels 24 h after staining with DilC, Figure 3.

DilC allowed visualization of attached cell and microcolonies where in pre-stained cultures more signal spots in the channel DilC were observed respect to spots in the DAPI channel. Additionally, they present varying sizes and brightness. Their size ranges from spots smaller than DAPI ones to spots with a diameter up to many times the size of a DAPI spot, Figure 3. However, the diameter of these spots was not measured, as the script allows to define pixel sizes to be excluded.

## 7.2 Influence of lipophilic stain over bacterial attachment to pyrite surfaces and comparison between image analysis software.

The growth of the planktonic cell population was assessed through cell density quantification, where no significant differences between unstained and DiIC pre-stained cells were measured, indistinctively of the media used for inocula growth, Figure 4.

The attachment of DAPI stained and DiIC pre-stained *L. ferrooxidans*[T] cells onto the pyrite surface was compared through quantification by software of EFM images, Figure 5 and Figure 6, in order to assess differences in attachment as a result of pre-staining with the lipophilic stain DiIC. Quantification of the attached population is necessary, even though differences can be apparent just by sight using DNA stains, since the heterogeneous distribution of bacteria on the pyrite surface requires a large number of grains to be analyzed, in order to obtain a representative model of the BF development.

In cultures inoculated with iron (II) grown cells, differences in the quantified signal spots per unit of pyrite surface were measured in the DAPI channel, between DiIC pre-stained and DAPI stained cultures. more DAPI signal spots per unit of pyrite surface were quantified than for DiIC pre-stained cultures, Figure 7 (D). At 120 h the average value obtained for the ratio was 1.23, indicating that the DAPI signal counts are similar between the two conditions, however no tendency in the value of the ratio was obtained, further assessment of the BF development in time would be necessary to assert if after 120 h the quantified signal spots in the DAPI channel between DiIC pre-stained and DAPI stained cultures tends to be similar.

In DiIC pre-stained cultures the quantified signal spots per unit of pyrite surface area in the DiIC channel, where greater than the quantified signal spots in the DAPI channel, Figure 7 (E). Interestingly, at 24 h, 48 h, 72 h and 96 h the ratio between DiIC signal count and DAPI signal count tends to 2, while at 120 h the value of the ratio abruptly increases indicating that there are 3.3 times more DiIC signal spots than DAPI signal spots.

In cultures inoculated with pyrite grown cells, differences in the quantified signal spots in the DAPI channel between DiIC pre-stained and DAPI stained cultures can be seen at 24 h, 48 h, and 72 h, where for DiIC pre-stained cultures, the results indicate that more DAPI signal spots per unite of pyrite surface area were quantified than for DAPI stained cultures, Figure 8 (D). At 120 h the average value obtained for the ratio was 0.96, indicating that the DAPI signal counts were similar between the two conditions, however no tendency in the value of the ratio was obtained, further assessment of the BF development in time is necessary to assert if past the 120 h the quantified signal spots in the DAPI channel between DiIC pre-stained and DAPI stained cultures tends to be similar.

For cultures inoculated with pyrite grown cells, in DiIC pre-stained cultures the quantified signal spots per unit of pyrite surface area in the DiIC channel, where greater than the quantified signal spots per unit of pyrite surface area in the DAPI channel at 24 h, 48 h and 72 h, Figure 8 (E). Interestingly, the ratio decreased linearly with time. At 96 h the ratio between DiIC signal count and DAPI signal count was 1.02, while at 120 h the value of the ratio is 0.81, indicating that more DAPI signal spots were quantified than DiIC

signal spots. This reduction on the ratio is caused by a reduction in the DiIC signal spots, together with a rise of the DAPI signal spots. The first could be caused by on the size and brightness of the DiIC signal spots, making them harder for the software to recognize, as dimmer signal spots would be filtered by the threshold, a program that allows to set a threshold, only in the regions where pyrite grains are present, could allow for an accurate recognition of these signal spots in the DiIC channel. The second is caused by the multiplication of the BF population.

When comparing cultures inoculated with pyrite grown cells to cultures inoculated with iron (II) grown cells, significant differences in the quantified signal spots for the DAPI channel were measured, for almost all selected times, irrespective of DiIC pre-staining. Results indicate that more signal spots per mm$^2$ of pyrite surface were found in samples of *L. ferrooxidans*[T] cultures where pyrite grown cells were used as inoculum, Figure 8 (A, B and C). These differences in growth as a result of the media used for growing the inocula are clearly seen in DAPI stained cultures where significative differences are seen in all points except at 72 h, Figure 8 (A). Also, significative differences between signal counts per unit of pyrite surface area were measured for DiIC pre-stained cultures in the DAPI channel at 48 h, 96 h and 120 h, Figure 8 (B). These differences were not seen when comparing planktonic cells population, indicating that the BF population growth is greater in cultures inoculated with pyrite grown cells. Pyrite grown cells have already expressed genes necessary for survival (e.g., to enhanced levels of ROS), growth and attachment in pyrite media (Bellenberg et al., 2015), therefore faster growth is expected compared to iron (II) grown cultures, that would experiment a lag phase as a result of the media change.

In DiIC pre-stained cultures in the DiIC channel significative differences between the signal counts per $mm^2$ of pyrite surface in pyrite grown and iron (II) grown inocula were obtained 48 h and 96 h, Figure 8 (C), therefore more data would be necessary to assert if a difference exist in the DiIC signal counts per area as a result of the media used for inocula growth, or if in the DiIC channel signal spots are not affect by the media inocula is growth. For cultures inoculated with pyrite grown cells the ratio between the recognized signal spots per unit of pyrite surface area in the DAPI channel for cultures inoculated with unstained and DiIC pre-stained cells was closer to one in comparison to cultures inoculated with iron (II) grown cells with more signal spots recognized for DiIC pre-stained cells, Figure 8 (D). Finally, the ratio between signal spots recognized for the DiIC channel and the DAPI channel declines for cultures inoculated with pyrite grown cells, Figure 8 (E).

Nowadays a great variety of open source and proprietary software for image analysis and image analysis tools exist, with different modules and applications. In order to analyze a vast database of BF images, finding efficient and flexible software for analysis is a necessary step towards automatization and big data image analysis. At least three approaches exist for analyzing an image obtained from a biological sample: 1) Developing a software specially for the required task 2) Buying a software produced by a developer 3) Using a public domain software. Each option comes with advantages and costs, leading researchers to use one or another. However, in order to know which is best for each case, or to compare results obtained between two software, comparisons using the same datasets have to be done. To achieve this, cell counts have been done using three software: 1) a custom-made script 2) Zen 3.0 software equipped with an

image analysis module, and 3) Fiji, Figure 9. Each software has different parameters and options for image analysis, and as a result, distinct estimations of the number of signal spots arise. However, Zen 3.0 was the software with a greater cell count for each image, especially when DiIC was quantified, Figure 9.

Zen 3.0 image analysis module allows to select filters, such as "Intensity maximum of channel DAPI", whose range sets based on the manually selected colonies, hence the range of the threshold is unique and optimized for each image allowing to recognize signal spots whose values for the selected filters are either wide or narrow. This dynamic threshold option that requires user intervention could explain that even though colonies outside pyrite grains are being filtered, more colonies are being recognized for each picture in comparison to Fiji and custom-script. Filtering of the colonies outside the pyrite grains was not performed in quantifications using Fiji, therefore quantification results were larger than those obtained by using custom-script where filtering of the colonies was done.

According to the quality of the image taken, definition of the colonies' edges, absence of colonies outside pyrite grains, and range of the channel intensity values, colonies could be easily identifiable, explaining similar colony counts between the three used software for the same dataset of images of *L. ferrooxidans*[T] BFs. Therefore, for images with a good signal, the selected software for analysis becomes irrelevant for the final quantification result.

47

## 7.3 Effect of external addition of HSL and DSF molecules.

Attachment and dispersion of *L. ferrooxidans*[T] and *L. ferriphilum*[T] cells was quantified using the custom-made script, as this technique was the less time consuming while simultaneously allowing for pyrite area quantification and filtering of colonies outside the pyrite grains.

In HSL external addition assays no differences in dispersion of *L. ferrooxidans*[T] or *L. ferriphilum*[T] cells were measured comparing to cultures with DMSO addition, Figure 10.

In attachment assays differences between the quantification results obtained between cultures with DMSO addition and cultures with no additions were measured, therefore all differences in cell attachment and BF dispersion were calculated comparing to cultures with DMSO addition. Additionally, a high standard deviation (SD) was obtained for the signal spots quantifications done for cultures with addition of HSL, this result can be explained by the variability of the quality of the images in this image set, as the signal spots in some images belonging to this set were not in focus or have variable intensity in the DAPI channel compared to the background signal noise, this results in an underestimation of colonies on the mineral surface.

Differences in attachment of *L. ferriphilum*[T] cells were measured when O-C14-HSL, C12 & O-C12-HSL and C14-HSL & O-C14-HSL was added, in comparison to control cultures with DMSO addition, Figure 11 (A). A reduced the number of attached colonies was measured when C12-HSL & O-C12-HSL, C14-HSL & O-C14-HSL or O-C14-HSL was externally added. Interestingly, the same mixtures of HSLs measured to reduce cell

attachment, enhanced BF dispersion, suggesting that the presence of these signaling molecules may favor a planktonic phenotype. Moreover, the capacity to inhibit BF formation can be specific, as observed for the effect of O-C14-HSL over *L. ferriphilum*[T] cells, or unspecific as observed for the effect of C12-HSL & O-C12-HSL and C14 & O-C14-HSL in both species, Figure 11 (B). Obviously, to assert if this effect is truly specific or unspecific further experiments using these HSLs would be necessary.

For DSF molecules external addition assays, significant differences between cultures with and without DMSO addition were measured at 4 h in attachment assays, Figure 12 (A), these differences were not observed in samples taken from cultures at other times, and no differences in attachment as a result of DSF or BDSF at 4 h were measured in comparison to cultures with DMSO addition. Therefore, the measured differences as a result of DSF or BDSF addition at 4h are not unequivocal, as they could be explained by the DMSO addition.

Upon DSF molecules addition, no changes in the pattern of dispersion or attachment onto the pyrite surface of *L. ferriphilum*[T] were observed. However, for assays with DSF addition three images were analyzed for each sample, while for assays with HSL addition thirteen images were quantified, the lack of significant differences found in DSF addition assays can be attributed to insufficient data points taken, therefore is necessary to repeat these experiments and to quantify bigger dataset of images in order to assert if attachment or dispersion is affected upon DSF addition.

**8 Conclusions.**

In this work datasets of different sizes were analyzed, while the size of the dataset is important for accurately representing BF development in time, not only the quantity of images analyzed is important, the quality of the images is also necessary for a correct recognition of the present colonies, adding another factor to take into account when analyzing BF images. This highlights the necessity for efficient protocols for BF staining and image acquisition. Even though a protocol for staining *L. ferrooxidans*[T] and *Acidiferrobacter* sp. SP3/III with DiIC was successfully used, the correlation between the number, size and position of the quantified signal spots for DiIC channel and DAPI channel has not been yet clarified, as a software for this purpose is necessary, future work is being currently done to stablish a spatial correlation between these two stains. Furthermore, it is necessary to study the colocalization between these two stains as some signal spots observed for DiIC do not colocalize with a DAPI signal spots and are smaller than the expected size for bacterial cell, these signal spots could indicate sites of contact but not attachment between the pyrite surface and the cells, where membrane vesicles could remain in the pyrite surface.

Although significant differences in colony quantification between unstained and pre-stained cultures were found, the use of lipophilic membrane dyes on acidophilic leaching organisms offers an interesting alternative to cell transformation for cell tracking purposes. This is of special importance as these organisms thrive in acidic environments and have been proven difficult to transform by conventional methods.

Depending on the quality available data and the user's necessities, a variety of software are available for BF quantification. When comparing the results obtained using different software it is necessary to take into account the filtering and threshold done by the software, the quality and quantity of the analyzed images, and the dye used for staining, as these parameters have an effect over the quantification results.

Finally, this BF analysis methodology was tested by quantifying changes in BF formation patterns as a result of the addition of the external signaling molecules HSLs and DSFs. Even though quantification of the available images was achieved for DSFs addition assays, the available data is insufficient to properly assess BF formation, as no significant differences were measured. For HSL addition assays it was possible to measure differences between treatments, indicating that the number of measures done for each condition were sufficient to assess BF formation.

## 9.References.

Axelrod, D. *Carbocyanine dye orientation in red cell membrane studied by microscopic fluorescence polarization.* Biophys J. 1979 Jun;26(3):557-73. doi: 10.1016/S0006-3495(79)85271-6.

Barber, C.E., Tang, J.L., Feng, J.X., Pan, M.Q., Wilson, T.J., Slater, H., Dow, J.M., Williams, P., & Daniels, M.J. 1997. *A novel regulatory system required for pathogenicity of Xanthomonas campestris is mediated by a small diffusible signal molecule.* Mol. Microbiol. 1997;24(3):555-566. doi: 10.1046/j.1365-2958.1997.3721736.x

Bellenberg, S., Díaz, M., Noël, N., Sand, W., Poetsch, A., Guiliani, N., & Vera, M. 2014. *Biofilm formation, communication and interactions of leaching bacteria during colonization of pyrite and sulfur surfaces.* Res. Microbiol. 165(9), 773–781. doi: https://doi.org/https://doi.org/10.1016/j.resmic.2014.08.006

Bellenberg, S., Barthen, R., Boretska, M., Zhang R., Sand W. & Vera M. 2015. *Manipulation of pyrite colonization and leaching by iron-oxidizing Acidithiobacillus species.* Appl Microbiol. Biotechnol., 99, 1435–1449. doi: https://doi.org/10.1007/s00253-014-6180-y

Bellenberg, S., Buetti-Dinh, A., Galli, V., Ilie, O., Herold, M., Christel, S., Boretska, M., Pivkin, IV., Wilmes, P., Sand, W., Vera, M., & Dopson, M. 2018. *Automated microscopic analysis of metal sulfide colonization by acidophilic microorganisms.* Appl. Environ. Microbiol. 84:e01835-18. doi: https://doi.org/10.1128/AEM.01835-18.

Bolte, S., Talbot, C., Boutte, Y., Catrice, O., Read, N., & Satiat-Jeunemaitre, B. 2004. *FM-dyes as experimental probes for dissecting vesicle trafficking in living plant cells.* J. Microsc. 214: 159–173.

Bosecker, K. 1997. *Bioleaching: metal solubilization by microorganisms.* FEMS Microbiol. Rev., 20 (3-4), 591-604. doi: 10.1111/j.1574-6976.1997.tb00340.x

Brierley, C.L., & Brierley, J.A. 2013. *Progress in bioleaching: part B: applications of microbial processes by the minerals industries.* Appl. Microbiol. Biotechnol., 97, 7543-52. doi:10.1007/s00253-013-5095-3

Christel, S., Herold, M., Bellenberg, S., El Hajjami, M., Buetti-Dinh, A., Pivkin, I.V., Sand, W., Wilmes, P., Poetsch, A., & Dopson, M. 2018. *Multiomics reveals the lifestyle of the acidophilic, mineral-oxidizing model species Leptospirillum ferriphilumT.* Appl. Environ. Microbiol. 84:e02091-17. https://doi.org/10.1128/AEM.02091-1

Cochilco. 2017a. *Chilean copper mining costs.* https://www.cochilco.cl/Presentaciones%20Ingls/Chilean%20Copper%20Mining%20Costs.pdf

Cochilco. 2017b. *Tendencias de usos y demanda de productos de cobre.*https://www.cochilco.cl/Mercado%20de%20Metales/Tendencias%20de%20usos%20y%20demanda%20de%20productos%20de%20cobre.pdf

Cochilco. 2019. *Reporte anual 2019.* https://consejominero.cl/wp-content/uploads/2020/04/Reporte-Anual-CM-2019.pdf

Coram, N.J., & Rawlings, D.E. 2002. *Molecular relationship between two groups of the genus Leptospirillum and the finding that Leptospirillum ferriphilum sp. nov. dominates South African commercial biooxidation tanks that operate at 40 °C.* Appl. Environ. Microbiol. 2002;68(2):838-845. doi: 10.1128/aem.68.2.838-845.2002

Crowson, P. 2012. *Some observations on copper yields and ore grades.* Resources Policy, 37.doi: 10.1016/j.resourpol.2011.12.004

Farah, C., Vera, M., Morin, D., Haras, D., Jerez, C.A., & Guiliani, N. 2005. *Evidence for a functional quorum-sensing type ai-1 system in the extremophilic bacterium Acidithiobacillus ferrooxidans.* Appl. Environ. Microbiol., 71 (11), 7033–7040.

Flemming, H., & Wingender, J. 2010. *The biofilm matrix.* Nat. Rev. Microbiol. 8, 623–633. doi: https://doi.org/10.1038/nrmicro2415

Flemming, H-C., Wingender, J., Szewzyk, U., Steinberg, P., Rice, S., & Kjelleberg, S. 2016. *Biofilms: An emergent form of bacterial life.* Nat. Rev. Microbiol., 14, 563-575. doi: 10.1038/nrmicro.2016.94

Gullapalli, R.R., Demirel, M.C., & Butler, P.J. 2008. Molecular dynamics simulations of DiI-C18(3) in a DPPC lipid bilayer. Phys. Chem. Chem. Phys., 10(24), 3548-3560. doi: https://doi.org/10.1039/b716979e

Goldstein, I., Hollerman, C., & Merrick, J.M. 1965. *Protein-carbohydrate interaction I. The interaction of polysaccharides with concanavalin A.* BBA-Gen Subjects 97: 68–76.

González, A., Bellenberg, S., Mamani, S., Ruiz, L., Echeverria, A., Soulère, L., Dontheau, A., Demergaso, C., Sand, W., Quenaeu, Y., Vera, M., & Guiliani, N. 2012. *HSL signaling molecules with a large acyl chain enhance biofilm formation on sulfur and metal sulfides by the bioleaching bacterium Acidithiobacillus ferrooxidans.* Appl. Microbiol. Biotechnol., 97. doi: https://doi.org/10.1007/s00253-012-4229-3

Harneit, K., Goksel, A., Kock, D., Klock, J-H., Gehrke, T., & Sand, W. 2006*. Adhesion to metal sulfide surfaces by cells of Acidithiobacillus ferrooxidans, Acidithiobacillus thiooxidans and Leptospirillum ferrooxidans.* Hydrometallurgy, 83 (1), 245 254. doi: https://doi.org/10.1016/j.hydromet.2006.03.044

Inaba, Y., Banerjee, I., Kernan, T., & Banta, S. (2018). *Transposase-Mediated Chromosomal Integration of Exogenous Genes in Acidithiobacillus ferrooxidans.* Appl. Environ. Microbiol., 84(21). doi: https://doi.org/10.1128/AEM.01381-18

Issotta, F., Moya-Beltran, A., Mena, C., Covarrubias, P. C., Thyssen, C., Bellenberg, S., & Vera, M. 2018. *Insights into the biology of acidophilic members of the acidiferrobacteraceae family derived from comparative genomic analyses.* Res. Microbiol., 169 (10), 608 617. doi: https://doi.org/10.1016/j.resmic.2018.08.001

Johnson, B.D., & Hallberg, K.B. 2008. *Carbon, iron and sulfur metabolism in acidophilic micro-organisms.* In R. Poole (ed.), Adv. Microb. Physiol. pp 201-255. Academic Press, UK.

Johnson, B.D. 2015. *Biomining goes underground.* Nat. Geosci.,8,165-166. doi: 10.1038/ngeo2384

Lakshmanan, V.I., Roy R., & Ramachandran, V. 2016. *Innovative process development in metallurgical industry.* In V. Lakshmanan, R. Roy and V. Ramachandran (eds.), Springer, Switzerland.

Li, Q., & Sand, W. 2017. *Mechanical and chemical studies on EPS from Sulfobacillus thermosulfidooxidans: from planktonic to biofilm cells.* Colloids and Surfaces B: Biointerfaces, 153, 34–40. https://doi.org/https://doi.org/10.1016/j.colsurfb.2017.02.009

Li, Q., Yang, B., Zhu, J., Jiang, H., Li, J., Zhang, R., & Sand, W. 2018. *Comparative analysis of attachment to chalcopyrite of three mesophilic iron and/or sulfur-oxidizing acidophiles.* Minerals, 8, 406. doi: 10.3390/min8090406

Mackintosh, M. E. 1978. *Nitrogen fixation by thiobacillus ferrooxidans.* Microbiology, 105 (2), 215-218. doi: https://doi.org/10.1099/00221287-105-2-215

Mitchell, D., Harneit, K., Meyer, G., Sand, W., & Stackebrandt, E. 2004. *Systematic analysis of our culture collection for "genospecies" of Acidithiobacillus ferrooxidans Acidithiobacillus thiooxidans and Leptospirillum ferrooxidans.* In M. Tsezos, A. Hatzikoseyian, and E. Remoundaki (eds.), Biohydrometallurgy: A sustainable technology in evolution, Part II. pp 1369-1378. Proceedings of the international biohydrometallurgy symposium, IBS 2003, held in Athens, Hellas, September 14-19, 2003. Athens, Greece: National Technical University of Athens; 2004.

Nagy, A. 2013. *Lineage Marking.* R. Lanza and A. Atala (eds.), Handbook of Stem Cells. pp. 383-392. Elsevier, Canada

Ng, W-L., & Bassler, B.L. 2009. *Bacterial Quorum-Sensing Network Architectures.* Annu. Rev. Genet. 43(1), 197–222. doi: https://doi.org/10.1146/annurev-genet-102108-134304

Nicola, A.M., Frases, S., & Casadevall, A. 2009. *Lipophilic Dye Staining of Cryptococcus neoformans Extracellular Vesicles and Capsule.* Eukaryot. Cell, 8(9), 1373–1380. doi: https://doi.org/10.1128/EC.00044-09

Rawlings, D.E. (2002). *Heavy metal mining using microbes.* Annu. Rev. Microbiol. 56 (1), 65-91. doi: 10.1146/annurev.micro.56.012302.161052

Rohwerder, T., Gehrke, T., Kinzler, K., & Sand, W. (2003). *Bioleaching review part A: Progress in bioleaching: Fundamentals and mechanisms of bacterial metal sulfide oxidation.* Appl. Microbiol. Biotechnol. 63: 239-48. doi: 10.1007/s00253-003-1448-7

Ryan, R., & Dow, J. 2011. *Communication with a growing family: diffusible signal factor (dsf) signaling in bacteria.* Trends Microbiol. 19 (3), 145–152. doi: 10.1016/j.tim.2010.12.003

Sand, W., Rohde, K., Sobotke, B., & Zenneck, C. 1992. *Evaluation of Leptospirillum ferrooxidans for leaching.* Appl. Environ. Microbiol. 58, 85-92. doi: 10.1128/AEM.58.1.85-92.1992

Sand, W., Gehrke, T., Jozsa, P-G., & Schippers, A. 2001. *(bio)chemistry of bacterial leaching—direct vs. indirect bioleaching.* Hydrometallurgy. 59 (2), 159-175. doi: https://doi.org/10.1016/S0304-386X(00)00180-8

Sand, W., Gehrke, T., Hallmann, R., & Schippers, A. 2004. *Sulfur chemistry, biofilm, and the (in)direct attack mechanism a critical evaluation of bacterial leaching.* Appl. Microbiol. Biotechnol.43, 961-966.

Sand, W., & Gehrke, T. 2006. *Extracellular polymeric substances mediate bioleaching/biocorrosion via interfacial processes involving iron(iii) ions and acidophilic bacteria.* Res. Microbiol. 157, 49-56. doi: 10.1016/ j.resmic.2005.07.012

Simate, G.S., & Ndlovu, S. 2014. *Acid mine drainage: Challenges and opportunities.* J. Environ. Chem. Eng. 2 (3), 1785-1803. doi: https://doi.org/10.1016/j.jece.2014.07.021

Tayebi-Khorami, M., Edraki, M., Corder, G., & Golev, A. 2019. *Re-thinking mining waste through an integrative approach led by circular economy aspirations.* Minerals, 9, 286. doi: 10.3390/min9050286

Wang, L-H., He, Y., Gao, Y., Wu, J.E., Dong, Y-H., He, C., Su, X.W., Weng, L-X., Xu, J-L., Tay, L., Fang, R.X., & Zhang, L.H. 2004. *A bacterial cell–cell communication signal with crosskingdom structural analogues.* Mol. Microbiol., 51 (3), 903-912. doi: 10.1046/j.1365-2958.2003.03883.x

Watling, H. 2016. *Microbiological advances in biohydrometallurgy.* Minerals,6, 49. doi: 10.3390/min6020049

Watson, W. T., Minogue, T. D., Val, D. L., von Bodman, S. B., & Churchill, M. E. A. 2002. Structural Basis and Specificity of Acyl-Homoserine Lactone Signal Production in Bacterial Quorum Sensing. Molecular Cell, 9(3), 685–694. doi: https://doi.org/https://doi.org/10.1016/S1097-2765(02)00480-X

Wiederschain, G.Y. 2011. *The Molecular Probes handbook. A guide to fluorescent probes and labeling technologies.* Biochemistry. *76,* 1276 (2011). doi: https://doi.org/10.1134/S0006297911110101

Zhang, R.Y., Bellenberg, S., Neu, T., Sand, W., & Vera, M. 2016. *The biofilm lifestyle of acidophilic metal/sulfur-oxidizing microorganisms.* P. Rampelotto (ed.), Biotechnology of Extremophiles: Advances and Challenges. pp 177-213. Springer International, Switzerland.

Zhang, R.Y., Neu, T.R., Bellenberg, S., Kuhlicke, U., Sand, W., & Vera, M. 2015. *A lectin study of archaeal glycoconjugates during bioleaching.* Microb. Biotechnol. 8: 448-461. doi:10.1111/1751-7915.12188

Zhu, X., Li, J., & Wadsworth, M. E. 1994. *Characterization of surface layers formed during pyrite oxidation. Colloids Surface A.* doi: https://doi.org/10.1016/0927-7757(94)02935-0